Department of Biotechnology and Chemical Technology

Fault tolerant model predictive control (FTMPC) of the BioGrate boiler

Jukka Kortela

Aalto University

DOCTORAL DISSERTATIONS

Aalto University publication series
DOCTORAL DISSERTATIONS 20/2015

Fault tolerant model predictive control (FTMPC) of the BioGrate boiler

Jukka Kortela

Doctoral dissertation for the degree of Doctor of Science in Technology to be presented with due permission of the School of Chemical Technology for public examination and debate in Auditorium KE2 (Komppa Auditorium) at the Aalto University School of Chemical Technology (Espoo, Finland) on the 13th of February, 2015, at 12 noon.

Aalto University
School of Chemical Technology
Department of Biotechnology and Chemical Technology

Supervising professor
Prof. Sirkka-Liisa Jämsä-Jounela

Preliminary examiners
Prof. Carlos Bordons, University of Seville, Spain
Prof. Jero Ahola, Lappeenranta University of Technology, Finland

Opponents
Prof. Carlos Bordons, University of Seville, Spain
Prof. Matti Vilkko, Tampere University of Technology, Finland

Aalto University publication series
DOCTORAL DISSERTATIONS 20/2015

Kansi: Jussi Timonen, www.jussitimonen.com

ISBN 978-952-60-6079-8 (printed)
ISBN 978-952-60-6080-4 (pdf)
ISSN-L 1799-4934
ISSN 1799-4934 (printed)
ISSN 1799-4942 (pdf)
http://urn.fi/URN:ISBN:978-952-60-6080-4

Unigrafia Oy
Helsinki 2015

Finland

441 697
Printed matter

Aalto University
Aalto University, P.O. Box 11000, FI-00076 Aalto www.aalto.fi

Abstract

Author
Jukka Kortela

Name of the doctoral dissertation
Fault tolerant model predictive control (FTMPC) of the BioGrate boiler

Publisher School of Chemical Technology

Unit Department of Biotechnology and Chemical Technology

Series Aalto University publication series DOCTORAL DISSERTATIONS 20/2015

Field of research Kem-90 Process Control

Manuscript submitted 2 December 2014 **Date of the defence** 13 February 2015

Permission to publish granted (date) 21 January 2015 **Language** English

☐ **Monograph** ☒ **Article dissertation (summary + original articles)**

Abstract

Climate change and environmental concerns are forcing process industries to increase the share of sustainable resources in energy production. The utilization of biomass receives an increasing attention as a replacement for fossil fuels due to its wide availability and sustainability. However, the unpredictable variability of biomass properties, including moisture content, composition and heating value, results in disturbances, faults, and failures during the power plant operation, which creates additional barriers for a wider utilization of biomass.

This thesis focusses on the development of a fault tolerant model predictive control (FTMPC) scheme that addresses the challenges associated with the biomass utilization for power production in BioGrate boilers. The novelty of this scheme lies in the integration of soft-sensors measuring the unpredictable biomass properties with a fault accommodation mechanism.

The effectiveness of the developed FTMPC scheme is successfully tested with a dynamic simulator of the BioGrate boiler. This simulator is constructed using the industrial test data from the BioPower 5 CHP plant. In addition, industrial tests, conducted to evaluate the performance of the developed soft-sensors, confirm the prediction accuracy of the fuel moisture content and combustion power in the furnace. Subsequently, the economic evaluation of the soft-sensors integrated FTMPC scheme is presented.

Keywords fault tolerant control, model predictive control, biomass, fuel quality, fuel moisture, industrial process, combustion

ISBN (printed) 978-952-60-6079-8 **ISBN (pdf)** 978-952-60-6080-4

ISSN-L 1799-4934 **ISSN (printed)** 1799-4934 **ISSN (pdf)** 1799-4942

Location of publisher Helsinki **Location of printing** Helsinki **Year** 2015

Pages 141 **urn** http://urn.fi/URN:ISBN:978-952-60-6080-4

A! Aalto-yliopisto

Tiivistelmä

Aalto-yliopisto, PL 11000, 00076 Aalto www.aalto.fi

Tekijä
Jukka Kortela

Väitöskirjan nimi
Vikasietoinen malliprektiivinen säätö (FTMPC) BioGrate-kattilalle

Julkaisija Kemian tekniikan korkeakoulu

Yksikkö Biotekniikan ja kemian tekniikan laitos

Sarja Aalto University publication series DOCTORAL DISSERTATIONS 20/2015

Tutkimusala Kem-90 Prosessien ohjaus

Käsikirjoituksen pvm 02.12.2014 **Väitöspäivä** 13.02.2015

Julkaisuluvan myöntämispäivä 21.01.2015 **Kieli** Englanti

☐ **Monografia** ☒ **Yhdistelmäväitöskirja (yhteenveto-osa + erillisartikkelit)**

Tiivistelmä

Ilmastonmuutos ja ympäristökysymykset pakottavat prosessiteollisuutta kasvattamaan kestävien luonnonvarojen osuutta energiantuotannossa. Biomassa saa kasvavaa huomiota korvaavana vaihtoehtona fossiilisille polttoaineaineille johtuen sen hyvästä saatavuudesta ja hiilineutraalisuudesta. Kuitenkin biomassan ominaisuuksien arvaamaton vaihtelu, mukaan lukien kosteus, koostumus ja lämpöarvo, johtaa häiriöihin, vikoihin ja toimintahäiriöihin laitoksen operoinnissa, mikä luo esteitä biomassan laajemmalle hyödyntämiselle.

Tämä väitöskirja keskittyy vikasietoisen mallipredikitiivisen säätö (FTMPC) -järjestelmän kehittämiseen ottaen huomioon haasteet biomassan hyödyntämisessä energiantuotannossa BioGrate-kattiloilla. Uutta tässä järjestelmässä on soft-sensorien integrointi mittaamaan biomassan vaihtelevia ominaisuuksia yhdessä vikasietoisen menetelmän kanssa.

Kehitetyn FTMPC-järjestelmän tehokkuus on testattu käyttäen BioGrate-kattilan dynaamista simulaattoria, joka on tehty käyttäen hyväksi BioPower 5 CHP -laitoksen teollisia mittauksia. Lisäksi, teollisuudessa suoritetut koetulokset, joita käytettiin kehitettyjen soft-sensorien suorituskyvyn arvioimiseen vahvistavat, että polttoaineen kosteus ja palamisteho voidaan ennustaa hyvällä tarkkuudella. Tämän lisäksi kehitetyn FTMPC-järjestelmän taloudellinen merkitys on arvioitu väitöskirjassa.

Avainsanat vikasietoinen säätö, mallipredikitiivinen säätö, biomassa, polttoaineen laatu , polttoaineen kosteus, teollinen prosessi, palaminen

ISBN (painettu) 978-952-60-6079-8 **ISBN (pdf)** 978-952-60-6080-4

ISSN-L 1799-4934 **ISSN (painettu)** 1799-4934 **ISSN (pdf)** 1799-4942

Julkaisupaikka Helsinki **Painopaikka** Helsinki **Vuosi** 2015

Sivumäärä 141 **urn** http://urn.fi/URN:ISBN:978-952-60-6080-4

Preface

The research work presented in this thesis was carried out during the years 2008 - 2015 in the Research Group of Process Control and Automation at the Aalto University School of Chemical Technology. I would like to thank my supervisor Professor Sirkka-Liisa Jämsä-Jounela for her comprehensive academic guidance during the years and for her help in the writing of the thesis. Professor Raimo Ylinen is thanked for his valuable insights and advice on this thesis. Alexey Zakharov and Tushar Jain are specially thanked for the proof checking. The financial support from the Fortum Foundation, the Research Foundation of Helsinki University of Technology and the Walter Ahlström Foundation are gratefully acknowledged.

I would like to thank the pre-examiners of the thesis: Professor Carlos Bordons from the University of Seville, Spain and Professor Jero Ahola from the Lappeenranta University of Technology, Finland for their thorough pre-examination of this thesis and helpful comments and remarks.

The research presented in this thesis was done within the Energiakattilat ja lisäarvoa tuottavat erillispalvelut (Dynergia) and Integrated condition-based control and maintenance (ICBCOM) projects. I would like to thank all participants of the projects, and especially Juha Huotari for sharing his expertise.

I would like to thank all my colleagues in the laboratory for the team spirit and their valuable help with the thesis: Alexandre Boriouchkine, Aleksi Eskelinen, Octavio Pozo Garcia, Rinat Landman, Palash Sarkar, Vesa-Matti Tikkala, and Miao Yu.

I would also like to thank my parents Urpo and Marjatta for their continuous support over the years.

Finally, I would like to express my greatest gratitude to my wife, Henni Ahvenlampi, for her love and support.

Helsinki, January 23, 2015,

Jukka Kortela

Contents

List of Publications

This thesis consists of an overview and of the following publications which are referred to in the text by their Roman numerals.

I Kortela, J., Jämsä-Jounela, S.-L. (2012). Fuel-quality soft sensor using the dynamic superheater model for control strategy improvement of the BioPower 5 CHP plant. *International Journal of Electrical Power & Energy Systems*, **42** (1), 38-48 .

II Kortela, J., Jämsä-Jounela, S.-L. (2013). Fuel moisture soft-sensor and its validation for the industrial BioPower 5 CHP plant. *Applied Energy*, **105**, 66-74 .

III Kortela, J., Jämsä-Jounela, S.-L. (2015). Modeling and model predictive control of the BioPower combined heat and power (CHP) plant. *International Journal of Electrical Power & Energy Systems*, **65**, 453-462 .

IV Kortela, J., Jämsä-Jounela, S.-L. (2014). Model predictive control utilizing fuel and moisture soft-sensors for the BioPower 5 combined heat and power (CHP) plant. *Applied Energy*, **131**, 189-200 .

V Kortela, J., Jämsä-Jounela, S.-L. (2014). Fault-tolerant model predictive control (FTMPC) for the BioGrate boiler. *Applied Energy*, Submitted the 1st of December, 2014.

Author's Contribution

Publication I: "Fuel-quality soft sensor using the dynamic superheater model for control strategy improvement of the BioPower 5 CHP plant"

J. Kortela developed a method for estimating thermal decomposition of fuel and fuel moisture in a furnace, and the use of the method in the control strategy improvement of the BioPower 5 CHP plant. He also developed the simulator, performed all simulation tests, analyzed the results, and wrote the manuscript under the supervision of Prof. S.-L. Jämsä-Jounela.

Publication II: "Fuel moisture soft-sensor and its validation for the industrial BioPower 5 CHP plant"

J. Kortela developed a soft-sensor for the on-line monitoring of fuel moisture in a furnace. To verify the fuel moisture soft-sensor, the industrial tests were performed by J. Kortela, A. Boriouchkine, MW Power Oy, and Technical Research Centre of Finland (VTT). J. Kortela analyzed the results, and wrote the manuscript.

Publication III: "Modeling and model predictive control of the BioPower combined heat and power (CHP) plant"

J. Kortela developed the model predictive control (MPC) strategy, where the combustion model is based on the mass balances for water and dry fuel. In addition, he identified the models for the BioPower combined heat and power (CHP) plant. He also implemented the MPC code, performed all the simulation tests, analyzed the results, and wrote the manuscript.

Publication IV: "Model predictive control utilizing fuel and moisture soft-sensors for the BioPower 5 combined heat and power (CHP) plant"

J. Kortela developed the fuel bed height model for the BioGrate boiler. To verify the fuel bed height model, the industrial tests were performed by J. Kortela, A. Boriouchkine, MW Power Oy, and Technical Research Centre of Finland (VTT). In addition, J. Kortela developed the model predictive control (MPC) strategy that utilizes the fuel bed height model. He also performed all the simulation tests, analyzed the results, and wrote the manuscript.

Publication V: "Fault-tolerant model predictive control (FTMPC) for the BioGrate boiler"

The amount of fuel on the grate needs to be held close to the set point for the correct primary and secondary air ratio. Therefore the fuel bed height sensor is critical element in the control of the BioGrate boiler. J. Kortela developed the fault-tolerant model predictive control (FTMPC) to accommodate the fault in this fuel bed height sensor by active controller reconfiguration. He also implemented the FTMPC code, performed all the simulation tests, analyzed the results, and wrote the manuscript.

Nomenclature

w	zero-mean white-noise disturbance
σ	unit step function
β	coefficient for a dependence on the position of the moving grate
$\dot{m}$	mass flow, kg/s
$\dot{n}$	mass flow, mol/s
η_k	integrating disturbance states
Γ_d	measured disturbance prediction matrix
Γ_u	pulse response matrix
$\hat{\eta}$	disturbance estimation
$\hat{h}$	specific enthalpy estimation, MJ/kg
$\hat{x}$	state estimation
ν	residual
Φ	block Hankel matrix
ϕ	objective function
ϱ	specific density, $\mathrm{kg/m^3}$
ξ_k	zero-mean white-noise disturbance
A	state matrix of the state space model
A_d	unit diagonal matrix
B	input matrix of the state space model
b	bias

B_d	disturbance model
C	output matrix of the state space model
c	correction coefficient
C_η	zero matrix
C_i	specific heat capacity, J/molT
d	disturbance variable
E	disturbance matrix of the state space model
e	sensor fault vector
F	volume flow, m^3/s
h	specific enthalpy, MJ/kg
K	Kalman gain matrix
L_x	filter gain matrix for the state
L_η	filter gain matrix for the disturbance
N	moles needed to burn completely one kilogram of a fuel, mol/kg
n_i	moles, mol/kg
N_p	prediction horizon
N_w	prediction horizon
P	Error covariance matrix
p	pressure, N/m^2
Q	heat transfer, MJ/s
q	heat value, MJ/kg
Q_u	move supression factor weight matrix
Q_z	tracking error weight matrix
r	target variable
T	temperature, $^\circ\mathrm{C}$
t_d	time delay, s

u	manipulated variable
V	Covariance matrix
V	volume, m^3
v	zero-mean white-noise disturbance
w	fuel moisture content, %
w_i	mass fraction, %
X	volume, %
x	state
z	controlled variable

Subscripts

0	reference value
1	input
2	output
C	carbon
cr	convection and radiation
ds	dry solid
$EAir$	excess air
fg	flue gas
H	hydrogen
in	input
N	nitrogen
O	oxygen
qf	wet fuel
S	sulphur
s	steam
thd	thermal decomposition of fuel

wev water evaporation

wf dry fuel

Superscripts

g gas

1. Introduction

1.1 Background

The utilization of biomass fuel for heat and power production is growing due to an increasing demand for the replacement of fossil energy sources with renewable energy. As a result, the fast and the efficient control of power producing units becomes increasingly important in combustion of biomass to adapt the production to uncontrollable fluctuations in demand. (Edlund et al., 2011). However, the main challenges in biomass combustion control are caused by the unpredictable variability of the fuel quality, which results in disturbances, faults, and failures in the plant behavior and operations. In particular, this is true for the grate firing that is one of the main technologies currently used in biomass combustion (Leão et al., 2011).

The biomass combustion process is mainly disturbed by variations in the fuel properties, especially in the bulk density and the moisture (Gölles et al., 2014). Moreover, the biomass fuel is usually a blend of different fuel types, for example, spruce bark and dry woodchips which have a moisture content varying typically between 30% and 55% (Yin et al., 2008). This results in an uncertainty in the energy content of the fuel and complicates the operation of combustors (Hermansson et al., 2011). Therefore, the estimations of the combustion power and fuel moisture have been the main focus of the biomass combustion research.

The combustion power estimation in the furnace plays a key role for the control strategy design of power plants especially while compensating the disturbances in the fuel feed and the effect of fuel quality in power generation. However, there is no direct and reliable measurement either for the caloric value of a non-homogenous biomass or for the combustion power released in the burning process. Nevertheless, the combustion power can be derived from the thermal decomposition rate defined as the weight of biomass burned in a unit of time. The thermal decomposition rate can be estimated from the oxygen consumption, as suggested in the successful theoretical studies by Kortela and Lautala (1982) and confirmed by practical tests on a coal plant. In more details, the oxygen consumption is derived from the oxygen mass balance in the furnace, including the fuel composition, combustion air and the flue gases. The same method has later been applied to a grate boiler (Kortela and Marttinen, 1985) and has been used for the development of a model predictive control of a grate boiler (Gölles et al., 2014).

The fuel moisture content, which greatly affects the power produced by the boiler, requires to be estimated. Measuring the moisture content of the fuel is carried out on-line with direct and indirect methods. In indirect methods – that measure gas moisture content – the fuel moisture content can be derived by a mass balance, including the moisture content of the combustion air, the elementary composition of the fuel, and the composition of the combustion air (Nyström and Dahlquist, 2004). This time delay due to the transport time of the gas from the furnace to the measurement position can be measured within seconds, which broadens the possibility for successful disturbance compensation by the plant control (Hermansson et al., 2011). Fourier-transform infrared (FT-IR) technology is used in one successful indirect method of determining gas moisture content (Jaakkola et al., 1998). Hermansson et al. (2011) investigated a method that uses relative-humidity (RH) for measuring the moisture content in flue-gases from biomass combustion to indirectly determine the moisture content of the fuel. However, both methods require additional equipment and calibration.

The biomass boiler is a nonlinear, coupled multivariable system, and therefore, it needs to be controlled with an advanced method, like model predictive control (MPC). Several groups have worked on the application of model predictive control in medium- and large-scale biomass furnaces (Leskens et al., 2005; Paces et al., 2011). Recently, Bauer et al. (2010) have derived, for industrial control purposes, a simple but nonlinear model for biomass combustion that was later used by Gölles et al. (2011, 2014) to implement the model based control of a commercially available small-scale biomass boiler.

In addition to controlling the power production, the plant control has to maintain the optimal operating conditions in the furnace. According to the boiler design, for the complete combustion of biomass, the fuel bed height should be kept at the level to achieve the specified ratio between the primary and secondary air, and the amount of fuel in the furnace (Yin et al., 2008). In addition, the fuel bed height must be kept within admissible limits to avoid plant shutdowns. This has led to the development of the fuel bed height sensor for the BioPower 5 CHP process (Anon, 2014), based on the pressure drop measurement in the fuel layer (Jegoroff et al., 2013).

1.2 Research problem and asserted hypotheses

The main motivation for this thesis was to improve the overall efficiency of an industrial BioPower 5 CHP process. The advanced plant control needs to be developed to support fast and high magnitude changes in the power demand, whilst maintaining the optimal operating conditions in the furnace (Gölles et al., 2014). Model predictive control (MPC) has proven to be one of the most successful techniques of advanced control in process industries and was thus selected as a promising candidate for the control strategy problem.

The fault statistics of the BioPower 5 CHP plant was collected and examined by the authors in order to gather specific information on the faults in the BioGrate process. The study showed that nearly 90% of the losses were caused by inability of the control system to stabilize the plant in presence of unpredictable variations in the fuel quality and the fuel bed height. This supported the use of the latest developments of MPC, i.e. fault tolerant model predictive control (FTMPC) in the enhanced control system development.

The asserted hypothesis is that:

Availability and profitability of the BioPower 5 CHP process are improved by integration of fuel moisture content and combustion power estimations into a fault-tolerant model predictive control (FTMPC) scheme.

In order to prove the hypothesis, the following tasks are carried out:

Task 1 Design of the overall FTMPC scheme capable of compensating the fuel quality variations and the fuel bed height sensor fault in the BioPower 5 CHP process

Task 2 Development of a method for fuel moisture content estimation and combining it with the combustion power estimation

Task 3 Development of models for the BioGrate boiler

Task 4 Development of a fault tolerant MPC for the BioPower 5 CHP process

Task 5 Evaluation of the FTMPC performance with industrial tests and simulations

1.3 Content of the thesis

This thesis presents the development of fault tolerant MPC for the BioPower 5 CHP process. Chapter 2 presents the process and control strategy of the BioPower 5 CHP process. The state-of-the-art on modeling and control of grate boilers is given in Chapter 3. Chapter 4 presents the design of the FTMPC for the BioPower 5 CHP process. Chapter 5 details the performance validation of the FTMPC for the BioPower 5 CHP process. Firstly, the industrial testing environment is described, the validation of the fuel moisture soft-sensor and the developed process models are presented and subsequently the test results are reported. Secondly, the simulation environment of the BioPower 5 CHP process is outlined and the performance of the developed MPC is compared with the currently used control strategy of the BioPower 5 CHP process. Furthermore, the performance of the FTMPC is tested and discussed. In the final Chapter 6, the conclusions are drawn.

1.4 Contribution and novelty of the thesis

The main contribution of the thesis is the development of the fuel moisture soft-sensor, its combination with the combustion power method, and utilizing the methods in the control strategy improvement of the BioGrate boiler. Additionally, the novel fault tolerant model predictive control of the BioPower 5 CHP process has been developed to compensate the variations in the fuel quality and to tolerate the faults in the fuel bed height sensor. The novelty comes from incorporating the fuel moisture soft-sensor and the combustion power estimation into the fault tolerant MPC framework. The author also developed the simulator of the BioGrate boiler and the software to estimate the fuel moisture and the combustion power.

The contribution and novelty of this thesis have also been demonstrated in the publications. The Publication I presents an enhanced method for estimating fuel quality in a BioGrate process and the use of the method in control strategy improvement. The publication focuses on estimating the most essential process parameters: fuel moisture and thermal decomposition of fuel. The Publication II presents a soft-sensor for on-line monitoring of water evaporation rate in a furnace. To verify the soft-sensor, experiments were performed at the BioPower 5 CHP plant. The Publication III proposes an MPC that utilizes models of water evaporation and thermal decomposition of dry fuel to compensate for variations in fuel quality. In Publication IV, the fuel bed height model is developed for the BioGrate boiler and the improved MPC utilizing the fuel bed height sensor is proposed. The Publication V presents the FTMPC to accommodate the fault in the fuel bed height sensor by active controller reconfiguration.

2. Description of the BioGrate process and its control strategy

The BioPower 5 CHP process consists of two main parts: the furnace and the steam-water circuit. The heat used for steam generation is obtained by burning solid biomass fuel – consisting of bark, sawdust, and pellets – which is fed into the furnace together with combustion air. The heat of the flue gas is transfered by the heat exchangers to the steam-water circulation, where superheated steam is generated (Kallioniemi, 2008).

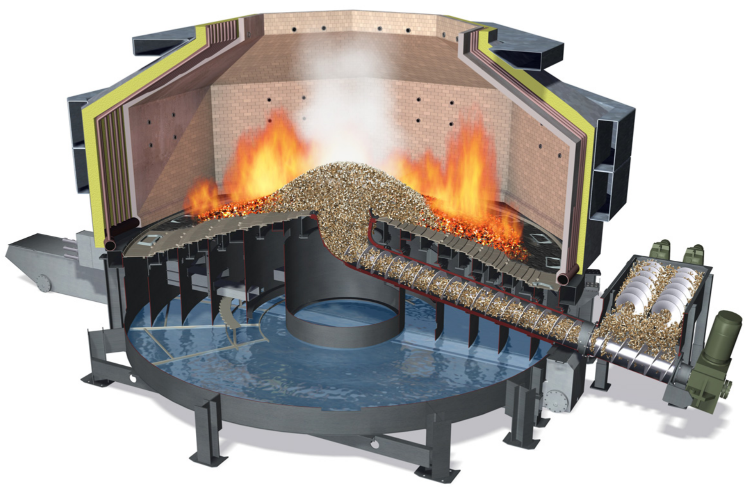

Figure 2.1. BioGrate, showing the stoker screw and the water-filled ash basin underneath the grate

In the BioGrate system (Anon, 2014), the fuel is fed onto the center of a grate from below through a stoker screw. The grate consists of alternate rotating and stationary concentric rings with the rotating rings alternately rotated clockwise and counter-clockwise by hydraulics. This design distributes the fuel evenly over the entire grate, with the burning fuel forming an even layer of the required thickness.

The moisture content of the wet fuel in the centre of the grate evaporates rapidly due to the heat of the surrounding burning fuel and the thermal radiation coming from the brick walls. The gasification and visible combustion of the gases and solid carbon takes place as the fuel moves to the periphery of the circular grate. At the edge of the grate, ash finally falls into a water-filled ash basin underneath the grate.

The primary air for combustion and the recirculation flue gas are fed from underneath the grate and they penetrate the fuel through the slots in the concentric rings. The secondary air is fed directly into the flame above the grate and the air distribution is controlled by dampers and speed-controlled fans. The gases released from biomass conversion on the grate and a small number of entrained fuel particles continue to combust in the freeboard, in which the secondary air supply plays a significant role in the mixing, burnout, and the formation of emissions. The design of the air supply system, the ratio between primary and secondary air, plays a key role in the efficient and complete combustion of biomass (Yin et al., 2008). In modern grate-fired boilers burning biomass, the split ratio of primary to secondary air is 40/60, which should be followed by a control design for the most efficient energy production. The overall excess air for most biomass fuels is normally set at 25% or above.

The essential components of the water-steam circuit are an economizer, a drum, an evaporator, and superheaters, as shown in Fig. 2.2. Feed water is pumped from a feed water tank into the boiler. First the water is led into the economizer (4), which is the last heat exchanger extracting the energy from the flue gas, and thus, improving the efficiency of the boiler. From the economizer, the heated feed water is transferred into the drum (5) and along downcomers into the bottom of the evaporator (6) through tubes that surround the boiler. From the evaporator tubes, the heated water and steam return back into the steam drum, where they are separated. The steam rises to the top of the steam drum and flows into the superheaters (7) where it heats up further and superheats. The superheated high-pressure steam (8) is then passed into the steam turbine, where electricity is generated.

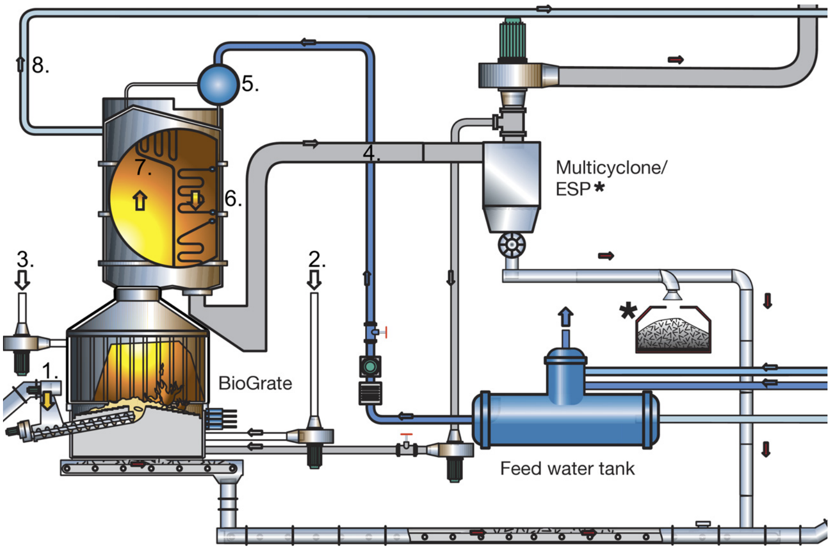

Figure 2.2. 1. Fuel, 2. Primary air, 3. Secondary air, 4. Economizer, 5. Drum, 6. Evaporator, 7. Superheaters, 8. Superheated steam

2.1 Control strategy of the BioGrate process

The main objective of the biopower plant is to produce power for the generator and for the hot water network. The difference between the consumed and produced power disturbs the pressure in the drum, and the control strategy equalize the steam production and consumption by controlling the drum pressure, which is achieved by manipulating the fuel and air supply to the furnace. Two feedforward and one ratio controllers attenuate variations during the transitions in the power demand as illustrated in Fig. 2.3.

In more details, the drum pressure control and the feedforward control, designed to compensate the variations of the superheated steam flow, determine the primary air flow setpoint. Based on the primary air flow, the ratio control computes the target level of the stoker speed to maintain the fuel feed according to the current combustion power level. The primary air defines the intensity of the pyrolysis and combustion, and the amount of the excess air (the secondary air) should follow the primary air to achieve the complete combustion. Thus, the feedforward controller is used to vary the secondary air proportionally to the primary air flow. However, the change in the fuel moisture content and the disturbances in the fuel feed are not taken into account in the control strategy, therefore causing oscillation in steam pressure.

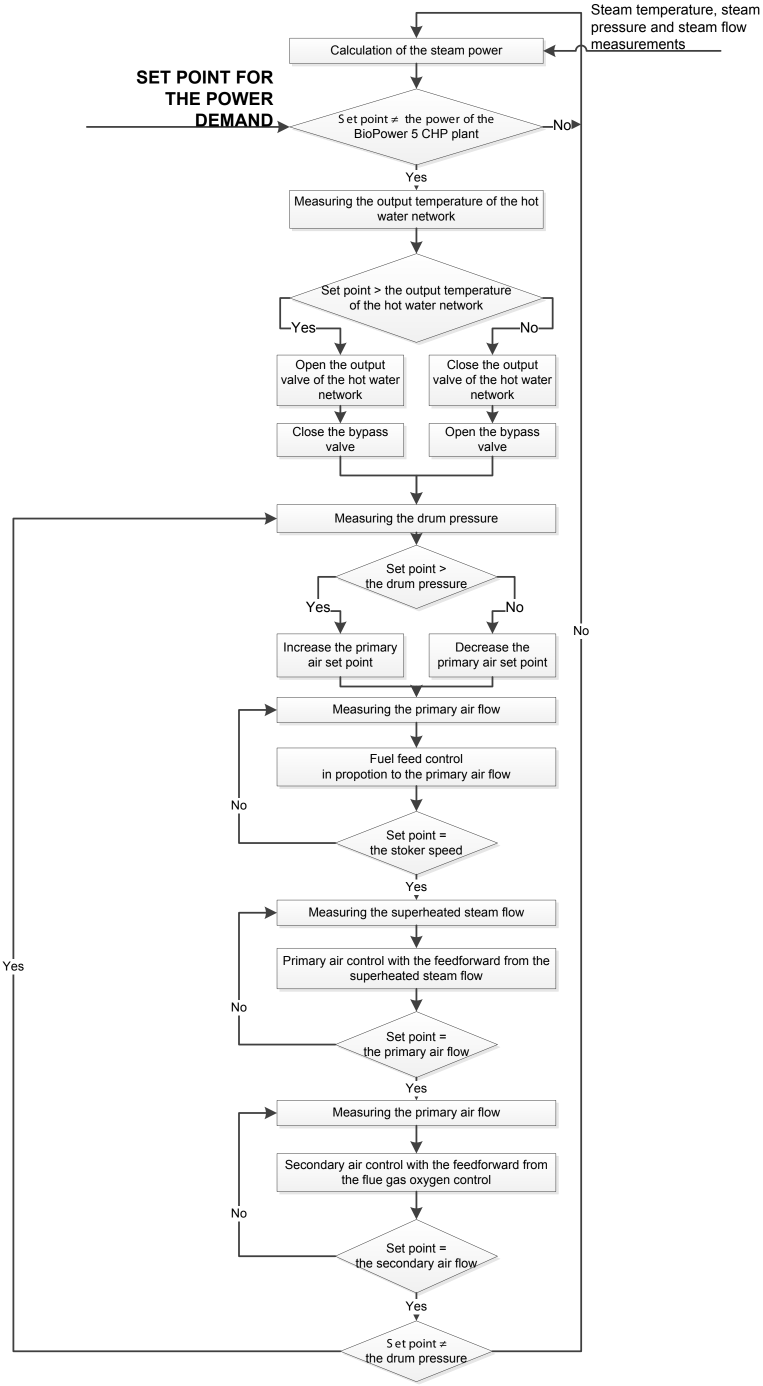

Figure 2.3. Current control strategy of the BioPower 5 CHP plant

3. Modeling and control of grate boilers; State-of-the-art

This chapter presents the state-of-the-art in modeling and control of grate boilers. In more details, the mechanistic modeling of grate boilers is briefly presented, the techniques for measuring the fuel moisture content are reviewed, and a survey on the control methods of grate boilers is presented.

3.1 Modeling of the grate combustion of biomass

As the basis for the modeling work, the effect of fuel properties on the combustion has been actively studied. Saastamoinen et al. (2000) studied the effects of the air flow rate, fuel moisture content, particle size, bed density, and wood type. Moisture did not have any noticeable effect on the maximum temperature in the bed when the moisture was less than 30 wt %. The velocity of the combustion front was found to be inversely proportional to the density of the fuel and specific heat of wood. Yang et al. (2003) conducted detailed mathematical simulations as well as experiments on the combustion of wood chips, and the incineration of simulated municipal solid wastes in a stationary bed. They concluded that the ignition time is influenced by both the devolatilization rate and the moisture content of the fuel. Furthermore, an increase in the fuel moisture shifts the combustion stoichiometry to a fuel-lean condition.

Similarly, Yang et al. (2005a) employed the mathematical model of a packed bed system to simulate the effects of the particle size, material density, bed porosity and the fuel calorific value on the combustion characteristics in terms of combustion rate, combustion stoichiometry, flue gas composition, and solid-phase temperature. They demonstrated that the combustion rate is determined by both the fuel particle size and the fuel density: smaller fuel particle sizes resulted in higher combustion rates due to the increased heat and mass transfer area and enhanced gas-phase mixing in the bed. The combustion front propagation velocity decreases as the biomass material density increases. Yang et al. (2005b) further investigated the effect of particle size on pinewood combustion in a packed bed and they concluded that both char burnout and fuel devolatilization occur at the same time in a bed of large particles.

As a conclusion from the previous studies, the particle size was found to have a strong effect on the combustion process. Johansson et al. (2007) investigated the use of a porous media approximation in the modeling of the fixed bed combustion of wood and concluded that the model is acceptable for the particle size below 2 cm. For modeling purposes, the combustion ongoing in separate particles has to be considered in more details when the particle size is large. Recently, Ström and Thunman (2013) presented a robust and computationally efficient particle submodel for use in computational fluid dynamics (CFD) simulations. Gómez et al. (2014) presented a bed compaction submodel to account for the local shrinkage of the bed fuel during the combustion.

The co-current combustion conditions were compared with the counter-current conditions by Thunman and Leckner (2001). In the case of the co-current combustion, the ignition of biofuel starts at the surface of the grate, and the heat generated at the bottom of the bed by char combustion is transferred along with the gas up through the bed. In the result, the air flow dries and devolatilizes fresh fuel, and combustion is possible with a moisture content of up to 70 or 80 %. In the case of the counter-current conditions, when the fuel is ignited from the top, such moisture content would be excessively high, since devolatilization and combustion occur in a narrow front. Further comparison of the co-current and counter-current fixed bed combustion of biofuel was given in (Thunman and Leckner, 2003). The results show that at steady co-current combustion, drying, devolatilization, and char combustion occur separately, whereas the three stages occur in a close proximity to each other during the entire counter-current combustion process.

Based on these findings, Bauer et al. (2010) derived a simplified furnace model suitable for control and optimization purposes. The simplified model is based on two separate mass balances for water and dry fuel in the bed. It was assumed in the model that the overall effect of the primary air flow rate on the thermal decomposition of dry fuel is proportional, as confirmed by many authors (van der Lans et al., 2000; Johansson et al., 2007; Blasi, 2000). The results obtained by Boriouchkine et al. (2014) also demonstrated that combustion dynamics is strongly dependent on the air flow. In addition, Bauer et al. (2010) assumed in their model that the water evaporation rate is mainly independent of the primary air flow, which was confirmed by the conducted experiments. The proposed model was verified by experiments at a pilot scale furnace with a horizontally moving grate.

3.2 Methods for determination of the moisture content in biomass

The moisture content of the fuel has to be determined with a delay within seconds to allow the control system to correctly adjust the combustion air supply and the fuel feed. However, the typical procedure, the manual analysis of the collected samples from each fuel batch delivered to the plant, is not accurate enough to predict the moisture content of the fuel entering the furnace. As an alternative, the fuel moisture content can be determined on-line by direct measurements or using indirect methods. The direct measurements include the use of dual-energy X-ray absorptiometry (DXA) (Nordell and Vikterlöf, 2000), near infrared spectroscopy (NIR) (Axrup et al., 2000), radio frequency (RF), microwave (Okamura and Zhang, 2000), and nuclear magnetic resonance (NMR) (Rosenberg et al., 2001) (Nyström and Dahlquist, 2004). Among these methods, NIR has been investigated the most as a promising method to analyze the fuel moisture content either by an automatic sampling on the delivery or in the fuel mix before it is injected into the furnace. However, these methods are not economically feasible for small-scale combustors as they demand measurement a set-up and calibration.

The fuel moisture content can be derived indirectly from the water mass balance in the furnace, involving the measurement of the flue gas moisture content, the composition of the combustion air and the elementary composition of the dry fuel. The only delay of the measurement signal in this setup is due to the transport time of the gas from the furnace to the measurement position. As a result, the fuel moisture can be estimated within seconds, which opens up the possibility for successful disturbance compensation by the plant control. The flue gas moisture content required by the method can be measured directly using, for example, the fourier-transform infrared (FT-IR) technology (Jaakkola et al., 1998) or calculated from the relative humidity (RH) of the flue gas (Hermansson et al., 2011).

Bak and Clausen (2002) have developed and interfaced a fibre-optic probe for an FT-IR instrument for simultaneous and rapid measurements of gas temperature and composition. The combined error in the gas temperature was equal to 3.5 °C (63% confidence level) which is critical to identify gas components. Jaakkola et al. (1998) investigated the feasibility of a transportable FT-IR gas analyzer for analyzing wet extractive stack gas and they reported a relative standard deviation of 4.1% for moisture content. However, FT-IR-based analysis has been reported to be sensitive to the absolute temperature, pressure, temperature gradients, and particles carried within the gas, complicating measurements carried out directly in the flue gas duct and weakening the usability of the method.

Another method for measuring the flue gas moisture content, using a relative-humidity (RH) sensor, was developed by Hermansson et al. (2011) with the aim of improving the accuracy level of indirect determination of moisture content of fuel in a biomass furnace. The method was tested on a laboratory scale multi-fuel CFB boiler, burning wood chips of approximately 42 w-% moisture content, and a grate furnace, burning saw dust of approximately 54 w-% moisture content. Accurate results were achieved by a prior cooling of the extracted flue gas stream to approximately 80 °C, which increased the RH of the flue gases. The results of the tests showed that the method predicts the moisture content of the biomass fuel in the furnace with a good precision (<4% error) after a calibration and that the method was able to detect variations in moisture content within seconds. However, in order to use this method, additional devices, measurements, and calibration are needed. In conclusion, both FT-IR and RH methods are too complicated and expensive to be used in a small-scale biograte process.

3.3 Combustion power and fuel moisture soft-sensors

The original method of Kortela and Lautala (1982) assumed a constant fuel moisture content, even though the relative ratio of oxygen in the flue gas is affected by the variations of the fuel moisture contents, which introduces an error to the estimation. Recently, the combustion power method was improved by Kortela and Jämsä-Jounela (2010) who estimated the fuel moisture content from the steady-state energy balance of the boiler involving the combustion power estimation. As a result, the oxygen mass balance calculations were corrected and the error of the combustion power estimation was removed. Furthermore, as the combustion power is computed from the thermal decomposition rate, the consideration of the fuel moisture content improves the accuracy of the calculations.

The method of Kortela and Jämsä-Jounela (2010) considered the heat-exchange in the whole steam-water circuit of the boiler. In Publication I, the combustion power and fuel moisture estimation methods were further improved by developing and employing a nonlinear superheater model. In more details, the internal energy and the moisture content of the flue gas have been considered to estimate the power of the heat transfer in the superheater. In the result, the delay of the fuel moisture estimation was greatly reduced as the secondary superheater has a much faster dynamics compared with the heat-exchange in the whole steam-water circuit. The method was tested by the industrial tests in Publication II.

3.4 Control of a grate boiler

The combustion power method developed by Kortela and Lautala (1982) was employed by many control strategies to compensate variations in the fuel quality. Based on the combustion power method, in the same publication Kortela and Lautala (1982) suggested a feed-forward control: adjusting the fuel feed flow according to the thermal decomposition rate to stabilize the amount of the fuel in the furnace. As a result, the effect of the feed disturbance on the generated steam pressure decreased to about one third of the original value, and the settling time decreased from 45 min to only 13 min. The same method has later been applied to a grate boiler (Kortela and Marttinen, 1985).

Lehtomäki et al. (1982) implemented the combustion power based control in a peat power plant. The effective heat value of peat varies from 1200 to 4600 MJ/m^3 due to the moisture, density, and the age of peat. Moreover, the volume feeders were used in the process, which caused uncertainty in the mass flow rate of the fuel. By introducing the combustion power based compensation to the process control, Lehtomäki et al. (1982) reduced the standard deviation of the flue gas oxygen content to as low as ± 0.1 %, which it made possible to lower the total air flow and to reduce the flue gas energy losses. Furthermore, the stabilized steam temperature reduced the thermal stress on superheaters and connected pipes.

As an alternative method to stabilize the furnace state, Paces et al. (2011) presented a method to decouple the control of the boiler load and the amount and the distribution of fuel on the grate. Compared with the combustion power approach, the proposed method required an additional measurement for the fuel bed height profile, which can be estimated from the pressure drop over the grate, gas concentrations, the temperature and/or radiation in the furnace. The simulation results have confirmed the ability of the proposed control method to smoothly perform the transitions during the power load changes.

Recently, the model predictive control has proven to be a successful method for controlling renewable fuel power plants. In particular, the benefits of MPC-based control over conventional multivariable control have been demonstrated by Leskens et al. (2005) at a grate boiler combusting municipal solid waste. Gölles et al. (2011, 2014) implemented and experimentally verified a model based control in a commercially available small-scale biomass boiler using the simplified first-principle model that has been discussed in Section 3.1. In more details, the mass of water in the water evaporation zone and the mass of dry fuel in the thermal decomposition zone on the grate are considered as the states of the simplified model and are estimated by an extended Kalman filter. Test results showed that the control was always able to provide the required power whereas the conventional control (PID control based on standard control strategies) could not tolerate a feed water temperature drop of more than 7 °C. In addition, the control was able to operate the plant with a lower excess oxygen content during the load drop and especially under partial load conditions. The better control of the residual oxygen and the control of the air ratio led to lower emissions and higher efficiencies. In addition, the model-based control was able to handle without difficulties a step-wise change in the fuel moisture content from 26% to 38% and vice versa.

Kortela and Jämsä-Jounela have presented a control based on the combustion power and fuel moisture content soft-sensors in Publication I and Publication III. This control was extended in Publication IV by employing the fuel bed height measurements, as it was originally suggested by Paces et al. (2011).

4. Fault tolerant model predictive control (FTMPC) for the BioGrate boiler

In this chapter, the development of FTMPC and its modules for the BioGrate boiler are presented. First, the FTMPC is introduced in Section 4.1. Second, the overall FTMPC strategy is described in Section 4.2. Methods to estimate the thermal decomposition of the dry fuel, and a soft-sensor to estimate the water evaporation in the furnace are outlined in Section 4.2.3.2. The dynamic models of the BioGrate boiler are detailed in Section 4.2.4. Section 4.2.5.1 presents the detection of faults in the fuel bed height sensor. Finally, the MPC of the BioGrate boiler is presented in Section 4.2.5.2 including the controller reconfiguration.

4.1 Introduction to FTMPC

During the last decades, the applications of fault detection and isolation (FDI), as well as model predictive control (MPC), have been among the most active research areas in the field of control, especially, in process industries. In particular, the diagnosis of equipment malfunctions and process faults is considered to be one of the most important actions in the process supervision (Frank et al., 2000). In order to tolerate faults while maintaining desirable stability and performance properties, the fault-tolerant control schemes (FTCS) have been developed (Zhang and Jiang, 2008).

In this thesis, the active fault tolerant control approach is considered, in which the diagnosed fault triggers the corrective actions, including the fault accommodation and the controller reconfiguration, as demonstrated in Fig. 4.1. The accommodation means that the FTCS uses the information provided by the FDI to obtain the compensated or corrected estimates of the state variables, measured values, and manipulated inputs, and appropriately modifies the inputs and/or outputs of the existing controller with no modifications in its internal working, as illustrated in Fig. 4.2. In

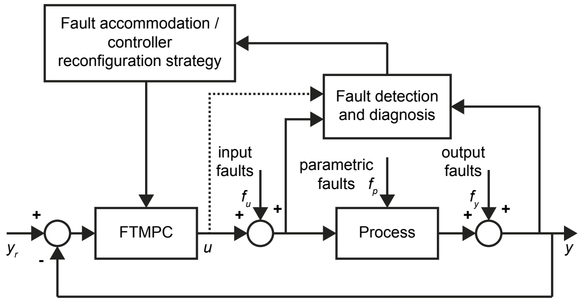

Figure 4.1. Schematic diagram for active fault tolerant MPC (Kettunen and Jämsä-Jounela, 2011)

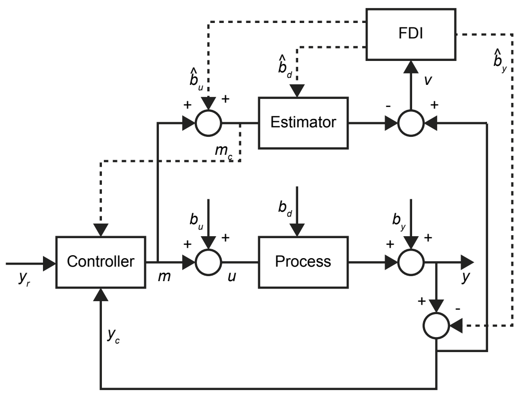

Figure 4.2. Fault-tolerant control scheme (FTCS) based on the generalized likelihood ratio (GLR) method (Prakash et al., 2002)

active FTCS, the reconfigured control parameters are frequently precomputed for all considered fault scenarios. In contrast, Zheng et al. (1997) used the theory of LMI to synthesize the control feedback as a function of "fault effect vectors", which are derived from the residual vector of the FDI.

Several applications of FTC in the process industry have been developed in the last decade. An active FTC strategy for the Naantali refinery de-aromatisation process was developed by Sourander et al. (2009) and extended by Kettunen and Jämsä-Jounela (2011). On the basis of the economic evaluation of just one feed grade, the annual estimated savings of the integrated FTMPC were predicted to be up to as much as USD 143 000.

In the active fault-tolerant control, fault detection plays a crucial role: without the proper detection of the faults, the corrective actions cannot be activated and the fault cannot be accommodated. Venkatasubramanian et al. (2003) divide faults into the following categories: structural changes in the process, actuator faults, sensor faults, gross parameter changes in the model, and external faults. Fault identification attempts to identify the fault type, the magnitude of the fault, and the direction of the fault in order to make it possible for the controller to counter the effect of the faults (Frank et al., 2000). The data based methods, including PCA (Li et al., 2000), PLS (Qin, 1998), and neural networks (Kohonen, 1990), as well as the model-based methods, such as parity equations (Haghani et al., 2014), observers and parameter estimation have been developed in the literature. For example, Prakash et al. (2002) implemented a fault detection and diagnosis method based on state estimation and integrated it to a FTCS. They showed that the FDD reformulated using the identified innovations form of state space model is able to isolate sensor faults as well as actuator faults. In addition, simulation studies of Patwardhan et al. (2006) showed that there is a need to deal with the abrupt changes in the unmeasured disturbances systematically in the FDI framework to improve its robustness.

4.2 FTMPC for the BioGrate boiler

4.2.1 Fault analysis of the BioGrate boiler operation

The control of the fuel bed height is a key element to stabilize the boiler operation. For complete combustion of biomass, the fuel bed height should be kept at the specified level to achieve the required ratio between the primary and secondary air. In addition, the fuel bed height should be kept within admissible limits to avoid plant shutdowns. The importance of the fuel bed height sensor is also confirmed by the results of the fault analysis for the BioGrate boiler operation in Fig. 4.3. In more details, the variations in the fuel quality and the amount of fuel on the bed propagate to the furnace temperature and combustion air flows, which are classified as faults in the boiler operation (40% of the losses) in Figure. The furnace temperature and combustion air flows further disturb the superheated steam temperature, causing the turbine shutdowns (47% of the losses). These two faults cover almost 90% of the economic losses at the plant.

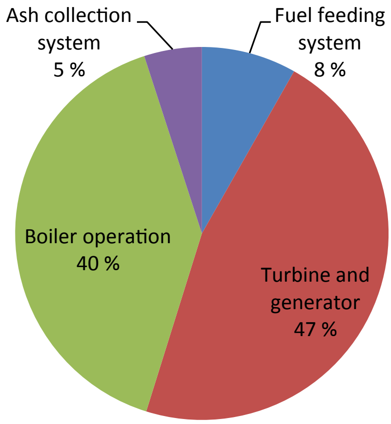

Figure 4.3. Economic loss distribution by the fault type

4.2.2 Overall structure of the FTMPC

The overall structure of the FTMPC follows the active FTC scheme, adjusting the plant control according to the fault diagnosis results. In more detail, two different MPC configurations have been developed for the cases of normal and faulty operations of the fuel bed height sensor. In the faultless mode, the MPC configuration is as follows: the primary air flow rate and the stoker speed are the manipulated variables (u); the moisture content in the fuel feed and the steam demand are the measured disturbances (d); and the fuel bed height and the steam pressure are the controlled variables (y). The fault is accommodated by employing an alternative estimation of the fuel bed height, which is based on the thermal decomposition rate. However, as the alternative estimation is less accurate, the control reconfiguration is also needed, shifting its focus to the combustion power control while the fuel height is given a low priority. Additionally, the fuel bed height is kept within the security limits in both configurations in order to avoid plant shutdowns.

In more details, the FTC scheme is presented in Fig. 4.4. The combustion power and fuel moisture soft-sensors are used to compensate the effect of the fuel quality variations. In particular, the fuel moisture estimation is considered by the MPC as a measured disturbance and is also used to estimate the amount of water in the furnace. Considering the combustion power as a model state enables rapid energy production level changes and improves the control performance during the transitions. In

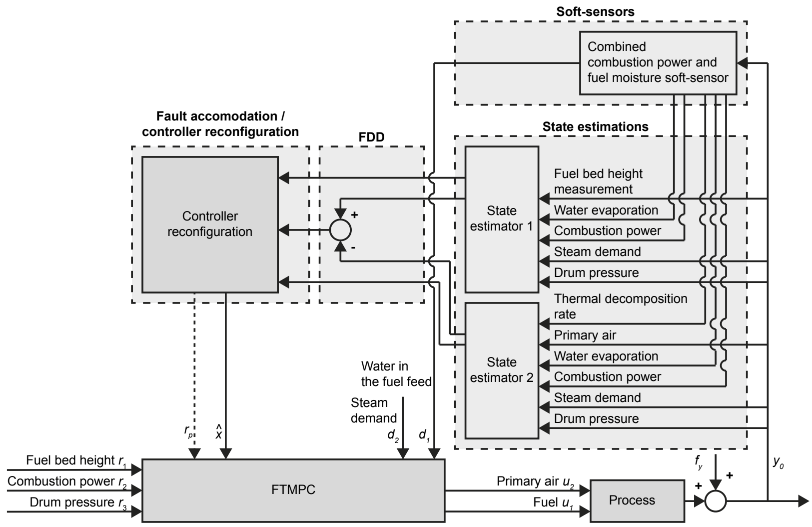

Figure 4.4. FTMPC of the BioGrate boiler

addition, the thermal decomposition rate is used in the calculations of the fuel bed height (estimator 2 in Fig. 4.4), which makes the fault detection and accommodation possible. According to the fault detection results, the decision on the control reconfiguration is made, which is then communicated to the fault accommodation and the FTMPC. Depending on the r_p value, the fault accommodation employs either the fuel bed height measurement or the thermal decomposition rate and the primary air flow for the MPC state estimation. Also, the switching takes place between the normal and the faulty configurations according to the r_p signal. The modules of the FTC are described in the following subsections in more details.

4.2.3 Combustion power and fuel moisture soft-sensors

This subsection presents the combustion power and fuel moisture soft sensors. The heat value of the fuel, involved in the energy balances utilized by the soft-sensor, is introduced first. The original combustion power method of (Kortela and Lautala, 1982), estimating the thermal decomposition rate based on the oxygen mass balance, is given in the second subsection. Next, the fuel moisture soft-sensor is presented, considering the energy balance for the superheater. Finally, a discussion on the synergy of the soft-sensors is provided, meaning the accuracy of both soft-sensors is improved by sharing information between them.

4.2.3.1 The heat value of dry and wet biomass

The heat value of a fuel can be determined by using the equation that has been derived from the heat values of the combustible components of fuel when they react with oxygen (Effenberger, 2000). The effective heat value of a dry fuel is (higher heat value):

$$\begin{aligned} q_{wf} &= 0.348 \cdot w_C + 0.938 \cdot w_H + 0.105 \cdot w_S \\ &\quad +0.063 \cdot w_N - 0.108 \cdot w_O [\text{MJ/kg}] \end{aligned} \tag{4.1}$$

where w_C is the mass fraction of carbon in the fuel (%), w_H is the mass fraction of hydrogen in the fuel (%), w_S is the mass fraction of sulfur in the fuel (%), w_N is the mass fraction of nitrogen in the fuel (%), and w_O the mass fraction of oxygen in the fuel (%). The effective heat value of a wet fuel (lower heat value) is obtained using the following equation:

$$q_{qf} = q_{wf} \cdot (1 - w/100) - 0.0244 \cdot w [\text{MJ/kg}] \tag{4.2}$$

where 0.0244 is the heat of vaporization of water, and w the moisture content of the wet fuel (%). In order to use Equation 4.1, the composition of typical fuels is given in Table 4.1.

Table 4.1. The composition of typical wood fuels burned in the Biopower 5 CHP plant

Fuel	Dry content (%)					Moisture (%)
	w_C	w_H	w_O	w_N	Ash	w
Pine	54.5	5.9	37.6	0.3	1.7	60
Spruce	50.6	5.9	40.2	0.5	2.8	60
Wood mix	50.4	6.2	42.5	0.5	0.4	50

4.2.3.2 Thermal decomposition of fuel and combustion power estimation

There are no direct online measurements available for the thermal decomposition of dry fuel. However, it can be estimated by utilizing combustion power soft-sensor. Oxygen consumption is a good measure of heat generation in such plants (Kortela and Lautala, 1982). As there is no direct measurement for the thermal decomposition of fuel, it is calculated indirectly by utilizing the flue gas oxygen content and the total air measurements.

The amount of oxygen needed for fuel combustion is determined from the reaction equations. Table 4.2 presents the moles of the fuel components per mass unit of the fuel. In summary, based on the amount of oxygen needed for a complete combustion of the different fuel components, minus the amount of oxygen in the fuel, the theoretical amount of oxygen

Table 4.2. Moles of the components of the fuel per unit mass

Comp.	Mass fraction (%)	M_i(g/mol)	n_i (mol/kg)
C	$w_c(1-w/100)$	12.011	$w_c(1-w/100)10/M_C$
H	$w_h(1-w/100)$	2.0158	$w_h(1-w/100)10/M_H$
S	$w_s(1-w/100)$	32.06	$w_s(1-w/100)10/M_S$
O	$w_o(1-w/100)$	31.9988	$w_o(1-w/100)10/M_O$
N	$w_n(1-w/100)$	28.01348	$w_n(1-w/100)10/M_N$
Water	w	18.0152	$10/M_W$

needed to completely burn one kilogram of fuel is given by:

$$N_{O_2}^g = n_C + 0.5 \cdot n_{H_2} + n_S - n_{O_2}[\text{mol/kg}] \tag{4.3}$$

Air consists mainly of oxygen and nitrogen (argon is often included in the nitrogen portion): 21 v-% oxygen and 79 v-% nitrogen. Theoretically, the corresponding amount of dry air needed is thus:

$$N_{Air} = N_{O_2}^g \cdot \frac{1}{0.21} = N_{O_2}^g \cdot 4.76[\text{mol/kg}] \tag{4.4}$$

Flue gases contain, in addition to combustion products, nitrogen N that comes with the combustion air. Flue gas calculations, therefore, include 3.76 times more nitrogen than the amount of oxygen necessary for complete combustion. Incombustible components, such as water, are included in the equations as such, meaning the flue gas flow for one kilogram of fuel is thus:

$$N_{fg} = n_C + n_{H_2} + n_S + 3.76 \cdot N_{O_2}^g + n_{N_2} + n_{H_2O}[\text{mol/kg}] \tag{4.5}$$

Similarly, the flue gas losses per kilogram of fuel are determined by:

$$\begin{aligned} q_{fg}^g = (&n_C C_{CO_2} + n_S C_{SO_2} + (n_{H_2O} + n_{H_2}) C_{H_2O} \\ &+ (3.76 \cdot N_{O_2}^g + n_{N_2}) C_N + (F_{Air}/(22.41 \cdot 10^{-3} \cdot \dot{m}_{gf}) \\ &- 4.76 \cdot N_{O_2}^g) C_{Air}) \cdot (T_{fg} - T_0)[\text{J/kg}] \end{aligned} \tag{4.6}$$

where C_i is the specific heat capacity of the component i (J/molT), F_{Air} is total air flow (m^3/s), $\dot{m}_{gf}$ is the thermal decomposition rate of the fuel (kg/s), T_{fg} is the temperature of the flue gas (°C), and T_0 the reference temperature (°C).

The combustion power of the BioGrate boiler is estimated using Equations 4.7 - 4.11. The total oxygen consumption is

$$\dot{n}_{O_2}^{tot} = 0.21 \cdot \dot{n}_{Air} - \frac{X_{O_2}}{100} \cdot \dot{n}_{fg}[mol/s] \tag{4.7}$$

where $\dot{n}_{O_2}^{tot}$ is total oxygen consumption (mol/s), $\dot{n}_{Air}$ is total air flow (mol/s), $X_{O_2}(t)$ is the oxygen content of the flue gas (%), and $\dot{n}_{fg}$ the flue gas flow (mol/s). The flue gas flow is:

$$\dot{n}_{fg} = \dot{m}_{gf} \cdot N_{fg} + \dot{n}_{Air} - 4.76 \cdot \dot{m}_{gf} \cdot N_{O_2}^{g}[\mathrm{mol/s}] \tag{4.8}$$

On the other hand, the oxygen consumption can also be presented in the following form:

$$\dot{n}_{O_2}^{tot} = \dot{m}_{gf} \cdot N_{O_2}^{g}[\mathrm{mol/s}] \tag{4.9}$$

and thus the thermal decomposition rate for the wet fuel is calculated as follows:

$$\dot{m}_{gf} = \frac{(0.21 - \frac{X_{O_2}}{100})\dot{n}_{Air}}{N_{O_2}^{g} + \frac{X_{O_2}}{100}(N_{fg} - 4.76 \cdot N_{O_2}^{g})}[\mathrm{kg/s}] \tag{4.10}$$

For the dry fuel, the calculations are done similarly. The denominator of Equation 4.10 is the amount of oxygen theoretically needed to burn one kilogram of fuel completely, added to the oxygen content in the flue gas. Finally, the net combustion power for a given fuel flow is:

$$Q = (q_{qf} - q_{fg}^{g} - q_{cr}) \cdot \dot{m}_{gf}[\mathrm{MW}] \tag{4.11}$$

where q_{cr} is convection and radiation losses (MJ/kg).

4.2.3.3 Fuel moisture soft-sensor

The developed fuel moisture soft-sensor estimates the water evaporation rate, from which the fuel moisture content can then be derived from the mass balance. The water evaporation affects the enthalpy of the secondary superheater, as the effective heat value of the fuel q_{qf} depends linearly on the fuel moisture content as shown by Equation 4.2. Therefore, by using the combustion power calculations presented in the previous Section 4.2.3.2, by considering the heat transferred into the secondary superheater, the fuel moisture content w is obtained by minimizing:

$$\min J(w) = \sum_{i=0}^{N_w} |h_{2,i} - \hat{h}_{2,i}|^2 \tag{4.12}$$

where N_w is the prediction horizon, $h_{2,i}$ is the measured steam enthalpy after the secondary superheater (MJ/kg), and $\hat{h}_{2,i}$ is the estimated steam enthalpy after the secondary superheater (MJ/kg). The model of the secondary superheater is defined as:

$$\frac{\mathrm{d}h_2}{\mathrm{d}t} = \frac{1}{\varrho V}(Q_s + \dot{m}_1 h_1 - \dot{m}_2 h_2)[\mathrm{MJ/(s \cdot kg)}] \tag{4.13}$$

where h_2 is the specific output enthalpy of the steam/water (MJ/kg), ϱ is the specific density of the steam/water (kg/m^3), V is the volume of the steam/water (m^3), $\dot{m}_1$ is the input steam/water flow (kg/s), h_1 is the specific input enthalpy of the steam/water (MJ/kg), and $\dot{m}_2$ is the output steam/water flow (kg/s).

The heat transfer from the flue gas to the metal walls in the presence of mixed convection and radiation heat transfer is (Lu, 1999; Lu and Hogg, 2000):

$$\begin{aligned} Q_{fg} = \alpha_{fg}\dot{m}_{fg}^{0.65}((T_{fg} - c_{fo} * T_{fo}) - T_{mt}) + \\ k_{fg}((T_{fg} - c_{fo} * T_{fo})^4 - T_{mt}^4)[\mathrm{MJ/s}] \end{aligned} \tag{4.14}$$

where α_{fg} is the convection heat transfer coefficient, c_{fo} is the correction coefficient, T_{fo} is the outlet flue gas temperature (°C), T_{mt} is the temperature of the metal tubes (°C), and k_{fg} is the radiation heat transfer coefficient. 0.65 is a constant for a bank of 10 or more tube rows (Incropera et al., 2007). Flue gas flow for the thermal decomposition rate of the fuel in Equation 4.10 is given by:

$$\dot{m}_{fg} = F_{Air} + \dot{m}_{gf}(N_{fg} - 4.76 \cdot N_{O_2}^g) \cdot 22.41 \cdot 10^{-3}[\mathrm{m}^3/\mathrm{s}] \tag{4.15}$$

where F_{Air} is the sum of the primary and secondary air flows (m^3/s), whereas the flue gas temperature is calculated using:

$$\begin{aligned} T_{fg} = \\ (q_{qf} + 0.21(F_{Air}/(22.41 \cdot 10^{-3} \cdot \dot{m}_{gf})C_{O_2} \\ +0.79(F_{Air}/(22.41 \cdot 10^{-3} \cdot \dot{m}_{gf})C_{N_2})/ \\ (n_C C_{CO_2} + n_S C_{SO_2} + (n_{H_2O} + \\ n_{H_2})C_{H_2O} + (3.76 \cdot N_{O_2}^g + n_{N_2})C_{N_2} + \\ 0.21 \cdot N_{EAir}C_{O_2} + 0.79 \cdot N_{EAir}C_{N_2})[°\mathrm{C}] \end{aligned} \tag{4.16}$$

where C_i is the specific heat capacity of the component i (J/molT), and the N_{EAir} excess air (mol/kg). The energy balance for the tube walls is:

$$\frac{\mathrm{d}T_{mt}}{\mathrm{d}t} = \frac{1}{m_m C_p}(Q_{fg} - Q_s)[\mathrm{K/s}] \tag{4.17}$$

where m_t is the mass of the metal tubes (kg), and C_p is the specific heat of the metal (MJ/kgK). The heat transfer from the metal walls to the steam/water in the presence of convection heat transfer (superheaters) is provided by:

$$Q_s = \alpha_c \dot{m}_2^{0.8}(T_{mt} - T)[\mathrm{MJ/s}] \tag{4.18}$$

where α_c is the convection heat transfer coefficient. The constant, 0.8, models the local Nusselt number for (hydrodynamically and thermally) fully developed turbulent flow by means of the Dittus-Boelter equation (Incropera et al., 2007; Winterton, 1998).

$$T = (T_1 + T_2)/2[^\circ\mathrm{C}] \tag{4.19}$$

where T_1 is the input steam/water temperature (°C) and T_2 the output steam/water temperature (°C).

4.2.3.4 The synergy of the combustion power and the fuel moisture soft-sensors

The drawback of the original combustion power method is that the fuel moisture is assumed to be constant and known. Indeed, the thermal decomposition estimation (4.10) involves the amount of flue gas for one kg of fuel N_{fg}, which is disturbed by the fuel moisture as seen from (4.5). Therefore, substituting the fuel moisture estimation to (4.5) allows to achieve accurate calculations resulting in the correct estimation of the thermal decomposition rate. In addition, the combustion power calculation from the thermal decomposition rate is also affected by the moisture content of the fuel, as it is involved in the fuel heat value equation (4.2).

On the other hand, the fuel moisture soft-sensor fits the estimated and the measured steam enthalpy after the secondary superheater (4.13), which includes the heat transfer from the flue gas to the steam computed according to Equations from (4.14) to (4.18). In particular, the thermal decomposition rate is utilized in Equations (4.15) and (4.16), defining the flue gas flow and the temperature. Therefore, the fuel moisture estimation is impossible without providing the thermal decomposition rate. In other words, the fuel moisture cannot be derived if the power transfered to the steam-water circuit is known, but the fuel consumption rate is not.

4.2.4 Dynamic model of the BioGrate boiler

The model describes the state of the furnace using the amount of dry fuel and the amount of water on the grate. The fuel moisture and the power demand are treated as measured disturbances, whereas the stoker speed and the primary air are considered as the inputs. The model predicts the fuel bed height, the combustion power and the drum pressure. The model, summarized in Fig. 4.5, consists of five submodels describing the dynamics of the fuel bed height, the amount of water in the furnace, the thermal decomposition rate, the combustion power and the drum pressure. The details of the submodels are presented in the following.

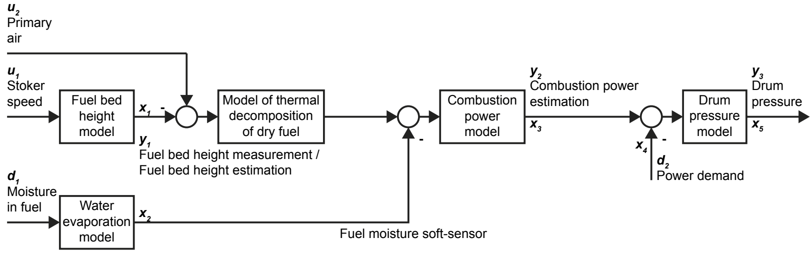

Figure 4.5. The models of the BioGrate boiler

4.2.4.1 *The model for the fuel bed height and the thermal decomposition rate*

Devolatilization and char burnout take place in the region marked "thermal decomposition zone" in Fig. 4.6. The dynamics of the dry biomass m_{ds} is based on the thermal decomposition rate of the fuel $\dot{m}_{thd}(t)$:

$$\frac{\mathrm{d}m_{ds}(t)}{\mathrm{d}t} = -\dot{m}_{thd}(t) + c_{ds,in}\dot{m}_{ds,in}(t)[\mathrm{kg/s}] \tag{4.20}$$

where $c_{ds,in}$ is the correction coefficient identified from the data.

In (Bauer et al., 2010), the effect of the primary air flow rate on the thermal decomposition of the fuel is proportional. In this work, the model was modified to describe the fuel bed height effect on the thermal decomposition rate:

$$\dot{m}_{thd} = c_{thd} \cdot \dot{m}_{pa} \cdot \beta_{thd} - c_{ds} \cdot m_{ds}[\mathrm{kg/s}] \tag{4.21}$$

where c_{thd} is the thermal decomposition rate coefficient, $\dot{m}_{pa}$ is the primary air flow rate (m^3/s), β_{thd} is the coefficient for a dependence on the position of the moving grate, c_{ds} is the fuel bed height coefficient, describing the mass of the fuel proportional to the density of the fuel. Nevertheless, with a constant fuel layer, the thermal decomposition rate increases linearly as the primary air flow rate increases, which is in agreement with (Bauer et al., 2010).

4.2.4.2 *The model of water evaporation*

In co-current combustion, most of the water evaporates in the region marked "moist fuel", as shown in Fig. 4.6. The energy for the water evaporation is mainly provided by the combustion of char near the surface of the grate, but in the BioGrate it is also provided by the heat of thermal radiation from the brick walls. The temperature near the bottom of the char layer is almost independent of the primary air flow, thus the water evaporation rate was mainly independent of the primary air flow as well

(Bauer et al., 2010). Therefore, the amount of water in the furnace is modeled as follows:

$$\frac{\mathrm{d}m_w(t)}{\mathrm{d}t} = -c_{wev}m_w(t)\beta_{wev}(t) + c_{w,in}\dot{m}_{w,in}(t-t_d)[\mathrm{kg/s}] \tag{4.22}$$

where $m_w(t)$ is the mass of the water in the evaporation zone (kg), β_{wev} is the coefficient for a dependence on the position from the center to the periphery of the moving grate, c_{wev} and $c_{w,in}$ are the model parameters estimated from the process data, and $\dot{m}_{w,in}$ the moisture in the fuel feed (kg/s). The time delay is defined as

$$t_d(t) = c_{td}\frac{m_w(t)}{\dot{m}_{ds,in}(t)}[\mathrm{s}] \tag{4.23}$$

where c_{td} is the delay coefficient, and $\dot{m}_{ds,in}(t)$ is the dry biomass flow rate (kg/s). The delay before the water starts to evaporate decreases as the amount of dry fuel increases.

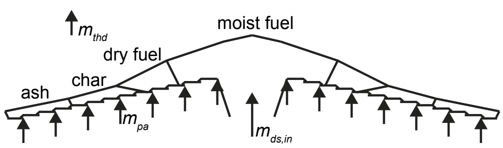

Figure 4.6. Thermal decomposition of fuel

4.2.4.3 Combustion power

The combustion power estimation considers the water evaporation and the thermal decomposition of the dry fuel separately:

$$\dot{Q} = q_{wf}\dot{m}_{thd} - 0.0244\dot{m}_{wev}[\mathrm{MJ/s}] \tag{4.24}$$

4.2.4.4 Combustion power

The drum level is kept constant by its controller, and therefore, the variations in the steam volume are neglected. Thus, the drum model is defined as (Åström and Bell, 2000):

$$\frac{\mathrm{d}p}{\mathrm{d}t} = \frac{1}{e}(\dot{Q} - \dot{m}_f(h_w - h_f) - \dot{m}_s(h_s - h_w)) \tag{4.25}$$

$$e \approx \varrho_w V_w \frac{\partial h_w}{\partial p} + m_m C_p \frac{\partial T_s}{\partial p} \tag{4.26}$$

where $\dot{Q}$ is the combustion power (MJ/s), $\dot{m}_f$ is the feed water flow (kg/s), h_w is the specific enthalpy of the water (MJ/kg), h_f is the specific enthalpy of the feed water (MJ/kg), $\dot{m}_s$ is the steam flow rate (kg/s), h_s is the specific enthalpy of the steam (MJ/kg), ϱ_w is the specific density of the water (kg/m^3), V_w is the volume of the water (m^3), m_m is the total mass of the metal tubes and the drum (kg), and C_p is the specific heat of the metal (MJ/kgK).

4.2.5 Controller reconfiguration

4.2.5.1 Model-based FDI for the BioGrate boiler

4.2.5.1.1 Generalized Model-based FDI strategy: A discrete time linear stochastic system is considered

$$x(k+1) = \Phi x(k) + \Gamma_u u(k) + \Gamma_w w(k) \tag{4.27}$$

$$y(k) = Cx(k) + v(k) \tag{4.28}$$

where $x \in R^n$ represents state variables, $u \in R^m$ represents manipulated inputs, $y \in R^r$ represents measured output, and $w \in R^q$ and $v \in R^r$ represent the state and the measurement noise with known covariance matrices Q and R respectively. If no fault occurs, the Kalman filter is used to obtain the optimal estimates of the state variables as follows:

$$\hat{x}(k|k-1) = \Phi\hat{x}(k-1|k-1) + \Gamma_u m(k-1); \hat{x}(0|0) = \hat{x}(0) \tag{4.29}$$

$$\hat{x}(k|k) = \hat{x}(k|k-1) + K(k)\nu(k) \tag{4.30}$$

$$\nu(k) = y(k) - C\hat{x}(k|k-1) \tag{4.31}$$

where $m(k)$ represents the controller output and $K(k)$ represents the Kalman gain matrix. Under a fault-free situation, the innovation $\nu(k)$ is a zero mean Gaussian white noise process with covariance matrix $V(k)$

$$V(k) = CP(k|k-1)C^T + R, \tag{4.32}$$

where the matrix $P(k|k-1)$ is obtained from the Kalman gain computations:

$$K(k) = P(k|k-1)C^T V^{-1}(k) \tag{4.33}$$

$$P(k|k) = (I - K(k))C)P(k|k-1) \tag{4.34}$$

$$P(k|k-1) = \Phi P(k-1|k-1)\Phi^T + \Gamma_w^T Q\Gamma_w. \tag{4.35}$$

If a bias of magnitude $b_{y,i}$ occurs at time instant t in the ith sensor, then the measurement output is given by

$$y(k) = Cx(k) + v(k) + b_{y,i}e_{y,i}\sigma(k-t) \tag{4.36}$$

where $e_{y,i}$ is a sensor fault vector with its ith element equal to unity and all other elements equal to zero, t represents the time of occurrence of the fault, and $\sigma(k-t)$ is a unit step function defined as

$$\sigma(k-t) = \begin{cases} 0 & \text{if } k < t \\ 1 & \text{if } k \geq t \end{cases} \tag{4.37}$$

The occurrence of a fault at time t is detected if the test statistic $\epsilon(N;t)$ exceeds the threshold:

$$\epsilon(N;t) = \sum_{k=t}^{t+N} \nu^T(k)V(k)^{-1}\nu(k) \tag{4.38}$$

4.2.5.1.2 Detection of faults in the fuel bed height sensor: Two state estimators in Fig. 4.4 utilize fuel moisture soft-sensor and combustion power estimations, steam, temperature, drum pressure measurements, and alternatively fuel bed height measurement and calculated fuel bed height to filter the states of the system, Fig. 4.5. In order to detect faults in the fuel bed height sensor, its filtered calculated value is compared with the filtered measurement. The fuel bed height can be expressed from the primary air flow rate and the thermal decomposition rate Equation (4.21) as follows:

$$m_{ds} = \frac{c_{thd} \cdot \dot{m}_{pa} \cdot \beta_{thd} - \dot{m}_{thd}}{c_{ds}} \tag{4.39}$$

If a bias of magnitude $b_{y,i}$ occurs at time instant t in the ith sensor, then the measurement output for this sensor is given by

$$y(k) = Cx(k) + v(k) + b_{y,i}e_{y,i}\sigma(k-t) \tag{4.40}$$

Furthermore, when a fuel bed height sensor fault occurs, the residual $\nu(k)$ and the two state fuel bed height estimates $\hat{x}(k|k)$ start to diverge from each other.

$$\nu(k) = y(k) - C\hat{x}(k|k-1) \tag{4.41}$$

$$\hat{x}(k|k) = \hat{x}(k|k-1) + K(k)\nu(k); \hat{x}(0|0) = \hat{x}(0) \tag{4.42}$$

The failure of the fuel bed height measurement is detected if the $RMSEP$ exceeds the detection threshold:

$$RMSEP = \sqrt{\frac{\sum_{i=1}^{n} |\hat{x}(i)_{1,1} - \hat{x}(i)_{1,2}|^2}{n}} \tag{4.43}$$

where n is the number of the samples in the test data set, $\hat{x}(i)_{1,1}$ is the estimated fuel bed height of the first MPC configuration, and $\hat{x}(i)_{1,2}$ the estimated fuel bed height of the second MPC configuration. The limit of detecting the faults is set above the normal disturbances of the states. Note that the fault isolation is implicitly done in the above fault detection procedure.

4.2.5.2 MPC of the BioGrate boiler

4.2.5.2.1 Linear discrete-time MPC: The MPC utilizes the linear state space system (Maciejowski, 2002):

$$\begin{aligned} x(k+1) &= Ax(k) + Bu(k) + Ed(k) \\ y(k) &= Cx(k) \end{aligned} \tag{4.44}$$

where A is the state matrix, B is the input matrix, E is the matrix for the measured disturbances, and C is the output matrix. According to (4.44), the k-step ahead prediction is formulated as:

$$y(k) = CA^k x(0) + \sum_{j=0}^{k-1} H(k-j)u(j) \tag{4.45}$$

where $\mathbf{H}(k-j)$ contains the impulse response coefficients. Therefore, using the Equation (4.45), the MPC optimization problem is:

$$\begin{aligned} \min \phi &= \frac{1}{2}\sum_{k=1}^{N_p} \|y(k) - r(k)\|_{Q_z}^2 + \frac{1}{2}\|\Delta u(k)\|_{Q_u}^2 \\ s.t. x(k+1) &= Ax(k) + Bu(k) + Ed(k), k = 0, 1, \ldots, N_p - 1 \\ y(k) &= Cx(k), k = 0, 1, \ldots, N_p \\ u_{\min} &\leq u(k) \leq u_{\max}, k = 0, 1, \ldots, N_p - 1 \\ \Delta u_{\min} &\leq \Delta u(k) \leq \Delta u_{\max}, k = 0, 1, \ldots, N_p - 1 \\ y_{\min} &\leq y(k) \leq y_{\max}, k = 1, 2, \ldots, N_p \end{aligned} \tag{4.46}$$

where r is the target value and $\Delta u(k) = u(k) - u(k-1)$.

The original system of Equation (4.44) is augmented with disturbance matrices to achieve the offset-free tracking in the presence of model-plant mismatch or unmeasured disturbances (Pannocchia and Rawlings, 2003).

$$\begin{bmatrix} x(k+1) \\ \eta(k+1) \end{bmatrix} = \begin{bmatrix} A & B_d \\ 0 & A_d \end{bmatrix} \begin{bmatrix} x(k) \\ \eta(k) \end{bmatrix} + \begin{bmatrix} B \\ 0 \end{bmatrix} u(k) + \begin{bmatrix} E \\ 0 \end{bmatrix} d(k) + \begin{bmatrix} w(k) \\ \xi(k) \end{bmatrix} \tag{4.47}$$

$$y(k) = \begin{bmatrix} C & C_\eta \end{bmatrix} \begin{bmatrix} x(k) \\ \eta(k) \end{bmatrix} + v(k) \tag{4.48}$$

The w_k and v_k are white noise disturbances with zero mean. Thus, the disturbances and the states of the system are estimated as follows:

$$\begin{bmatrix} \hat{x}(k|k) \\ \hat{\eta}(k|k) \end{bmatrix} = \begin{bmatrix} \hat{x}(k|k-1) \\ \hat{\eta}(k|k-1) \end{bmatrix} +$$

$$\begin{bmatrix} L_x \\ L_\eta \end{bmatrix} (y(k) - C\hat{x}(k|k-1) - C_\eta \hat{\eta}(k|k-1)) \tag{4.49}$$

and the state predictions of the augmented system of Equation 4.47 are obtained by:

$$\begin{bmatrix} \hat{x}(k+1|k) \\ \hat{\eta}(k+1|k) \end{bmatrix} = \begin{bmatrix} A & B_d \\ 0 & A_d \end{bmatrix} \begin{bmatrix} \hat{x}(k|k) \\ \hat{\eta}(k|k) \end{bmatrix} + \begin{bmatrix} B \\ 0 \end{bmatrix} u(k) + \begin{bmatrix} E \\ 0 \end{bmatrix} d(k) \tag{4.50}$$

Additional disturbances, η_k, are not controllable by the inputs u. However, since they are observable, their estimates are used to remove their influence from the controlled variables. The disturbance model is defined by choosing the matrices B_d and C_η. Since the additional disturbance modes introduced by disturbance are unstable, it is necessary to check the detectability of the augmented system. The augmented system (Equation (4.47)) is detectable if and only if the nonaugmented system (Equation (4.44)) is detectable, and the following condition holds:

$$\text{rank} \begin{bmatrix} I - A & -B_d \\ C & C_\eta \end{bmatrix} = n + n_\eta \tag{4.51}$$

In addition, if the system is augmented with a number of integrating disturbances n_η equal to the number of the measurements p ($n_\eta = p$) and if the closed-loop system is stable and constraints are not active at a steady state, there is zero offset in controlled variables.

4.2.5.2.2 MPC for the BioGrate boiler: Defining the inputs u, states x, outputs y and the measured disturbances d according to Fig. 4.5, the process models of the BioGrate are summarized as follows:

$$\frac{\mathrm{d}x_1}{\mathrm{d}t} = c_{ds}x_1 - c_{thd}\beta_{thd}u_2 + c_{ds,in}u_1 + w_2 \tag{4.52}$$

$$\frac{\mathrm{d}x_2}{\mathrm{d}t} = -c_{wev}\beta_{wev}x_2 + c_{w,in}d_1 + w_1 \tag{4.53}$$

$$\frac{\mathrm{d}x_3}{\mathrm{d}t} = -x_3 + q_{wf}(c_{thd}\beta_{thd}u_2 - c_{ds}x_1) - 0.0244c_{wev}\beta_{wev}x_2 + w_3 \tag{4.54}$$

$$\frac{\mathrm{d}x_4}{\mathrm{d}t} = -x_4 + d_2 \tag{4.55}$$

$$\frac{\mathrm{d}x_5}{\mathrm{d}t} = \frac{1}{e}(x_3 - x_4) + w_4 \tag{4.56}$$

$$y_1 = x_1 + v_1 \tag{4.57}$$

$$y_2 = x_3 + v_2 \tag{4.58}$$

$$y_3 = x_5 + v_3 \tag{4.59}$$

The following continuous-time state-space matrices are then discretized:

$$A = \begin{bmatrix} c_{ds} & 0 & 0 & 0 & 0 \\ 0 & -c_{wev}\beta_{wev} & 0 & 0 & 0 \\ -q_{wf} \cdot c_{ds} & -0.0244c_{wev}\beta_{wev} & -1 & 0 & 0 \\ 0 & 0 & 0 & -1 & 0 \\ 0 & 0 & 0.0020 & -0.0020 & 0 \end{bmatrix} \tag{4.60}$$

$$B = \begin{bmatrix} c_{ds,in} & -c_{thd}\beta_{thd} \\ 0 & 0 \\ 0 & q_{wf}c_{thd}\beta_{thd} \\ 0 & 0 \\ 0 & 0 \end{bmatrix} \tag{4.61}$$

$$E = \begin{bmatrix} 0 & 0 \\ c_{w,in} & 0 \\ 0 & 0 \\ 0 & 1 \\ 0 & 0 \end{bmatrix} \tag{4.62}$$

$$C = \begin{bmatrix} 1 & 0 & 0 & 0 & 0 \\ 0 & 0 & 1 & 0 & 0 \\ 0 & 0 & 0 & 0 & 1 \end{bmatrix} \tag{4.63}$$

The designed system uses an input disturbance model where $B_d = B$, A_d is the unit matrix, and C_η is the zero matrix. The set points r_2 and r_3 for the combustion power and the drum pressure directly result from procedural considerations. The set point for the combustion power is calculated according to the steam demand and the drum pressure is kept constant. An important process parameter is λ_{fb} describing the ratio of primary air fed to the fuel bed and minimum amount of the air necessary for a complete combustion of fuel. From the amount of dry fuel in the thermal decomposition zone, the input variable $\dot{m}_{pa}$ and the constant parameters (c_{thd}, β_{thd}, c_{ds}), the set point r_1 for the mass of dry fuel in the thermal decomposition zone is calculated.

$$m_{ds} = \frac{c_{thd} \cdot \dot{m}_{pa} \cdot \beta_{thd} - \dot{m}_{thd}}{c_{ds}} \tag{4.64}$$

Two different MPC configurations are developed for the process operating in two different modes, i.e. faultless or healthy mode and faulty mode.

In the faultless mode, the primary air flow rate and the stoker speed are the manipulated variables (u); the moisture content in the fuel feed and the steam demand are the measured disturbances (d); and the fuel bed height and the steam pressure are the controlled variables (y). While for the faulty mode, the controlled variables are modified: i.e. the output y is composed of the fuel bed height, the combustion power and the steam pressure. Once the fault is detected and isolated using the scheme described in Section 4.2.5.1, the controller is reconfigured from the healthy mode to the faulty mode.

5. Performance validation and economic evaluation of the FTMPC for the BioGrate boiler

In this chapter, the performance testing of the FTMPC and its different modules for the BioGrate boiler are presented. First, the test results of the method for determining the fuel moisture content and the thermal decomposition of dry fuel are described. Next, the identification and validation test results of the BioGrate combustion model are reported. Thirdly, the MPC control strategy is compared with the currently used control strategy in the BioPower 5 CHP plant and finally, the test results of the FTMPC for the BioGrate are presented and discussed.

5.1 Validation of the fuel moisture soft-sensor

In this section, the fuel moisture soft-sensor presented in Section 4.2.3.3 is validated with the industrial data. The moisture content of the fuel is changed stepwise with different amounts of dry fuel, the accuracy and dynamic performance of the soft-sensor with different moisture conditions are recorded, and the results are analyzed.

5.1.1 Description of the industrial testing environment

All the experiments for the validation of the fuel moisture soft-sensor were conducted at the BioPower 5 CHP plant, which produces 13.5 MW heat and 2.9 MW electricity. The plant utilizes the BioGrate combustion technology presented in Fig. 2.1. Two fuels were used to test the moisture soft-sensor: spruce bark with an average moisture content of 54% and a typical bark composition (carbon 51% , hydrogen 6.2%, nitrogen $< 0.2\%$, sulfur $< 0.2\%$, and ash 0.5%), and dry woodchips (spruce) with a moisture content of 20%. The moisture content was changed stepwise by feeding the dry biomass by means of the wheel loader onto the moving chain conveyor between the wet fuel through the extra feeding box. Three experiments were conducted to validate the fuel moisture soft sensor: In the first test, $5\mathrm{m}^3$ of dry biomass was fed onto the chain conveyor. In the second test, $10\mathrm{m}^3$ of dry biomass was fed. Finally, in the third test, $25\mathrm{m}^3$ of dry biomass was fed onto the chain conveyor.

The calculations presented in Section 4.2.3 were performed to obtain the current rate of water evaporation (fuel moisture soft-sensor value) and the current rate of thermal decomposition of the biomass. Measurement values of current air mass flows, current flue gas oxygen content, current steam temperatures, current steam flow and current steam pressure, as well as the results of the dry fuel analysis were used for calculations and all values were recorded every second. The following assumptions were however made: Excess air was used to enable the complete combustion of fuel, and the composition of the dry fuel was constant.

The ability of the method to determine the fuel moisture content was investigated as follows: Firstly, the effects of the fuel moisture on measurements utilized by the method were analyzed and discussed. Secondly, the accuracy of the method was tested by measuring the moisture content with the FT-IR analyzer in the extracted flue gas and by sampling of fuel feed every five minutes and comparing these measurements with the estimations of the fuel moisture soft-sensor. Lastly, the method was tested with transients by step tests utilizing the measured moisture content with the FT-IR analyzer.

5.1.2 Test results of the fuel moisture soft-sensor

In the following, the testing results of the fuel moisture soft-sensor are presented and discussed. The results of the first test are shown in Fig. 5.1 to Fig. 5.4. The top illustration of Fig. 5.1 shows the values calculated by the fuel moisture soft-sensor (thick line), the sampled fuel moisture (stars), and the fuel moisture calculated from the FT-IR measurements (thin line). Fig. 5.2 shows a more detailed description of the fuel moisture measurements. There was a delay of about 20 minutes between when the fuel moisture samples were taken before the stoker screw – as shown on the right side of Fig. 2.1 – and when the moisture content of the wet fuel in the centre of the grate was estimated by the fuel moisture soft-sensor and measured by the FT-IR analyzer. Therefore, the sampled fuel moisture was not directly comparable to the estimations of the fuel moisture soft-sensor and the measurements of the FT-IR analyzer measurements, but it gave an accurate measure of the moisture content in the fuel feed.

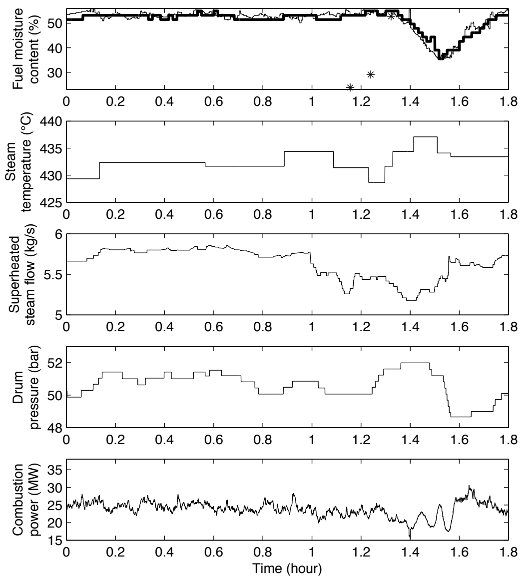

Figure 5.1. Boiler measurements during the first test, including measurements of superheated steam temperature, superheated steam flow, drum pressure, and combustion power responses to changes in the moisture content of the fuel flow. The top illustration shows the values calculated by the fuel moisture soft-sensor (thick line), the sampled fuel moisture (stars), and the fuel moisture calculated from the FT-IR measurement (thin line) for comparison. (Publication II)

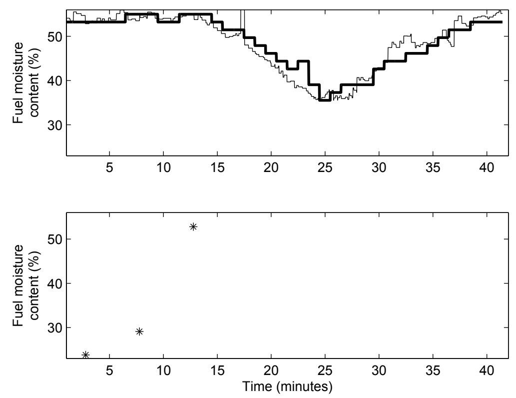

Figure 5.2. The fuel moisture soft-sensor (thick line) and the FT-IR measurement (thin line) responses to changes in the moisture content of fuel flow (the sampled fuel moisture). (Publication II)

As it can be seen from Fig. 5.1, the temperature after the secondary superheater and the drum pressure increased due to the addition of the dry fuel and the resulting greater combustion power. Primary air was used to

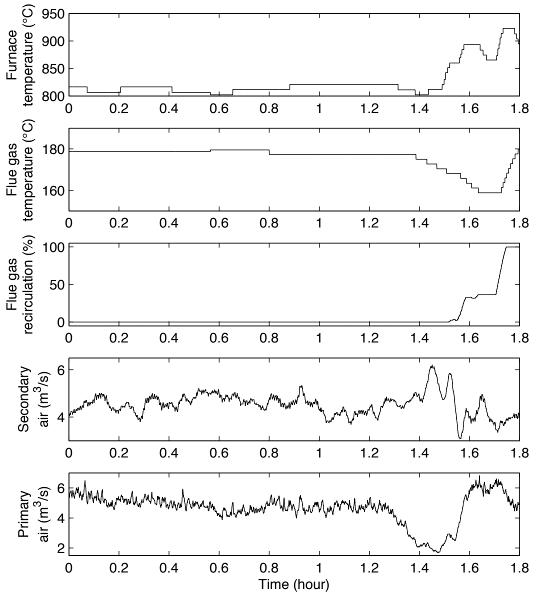

Figure 5.3. Boiler measurements during the first test, including furnace temperature, flue gas temperature, and changes in flue gas fan speed, secondary air flow, and primary air flow responses to changes in the moisture content of the fuel flow. (Publication II)

control the power of the boiler, and the primary air decreases due to the control action as a result of increases in the drum pressure, as shown in Fig. 5.3. As a result, the drum pressure and the secondary superheater temperature decreased when the superheated steam flow was kept at a high value. Furthermore, the flue gas oxygen content was kept at 4% using secondary air, i.e., secondary air varied almost independently from primary air and other variables. The temperature increases on the grate ring 10 were due to dry fuel that moved to the periphery of the grate increasing the furnace temperature as illustrated in Fig. 5.4. As a consequence, the flue gas circulation fan speed increased when the control action lowered the temperature.

The accuracy of the fuel moisture soft-sensor was investigated during the three tests by sampling fuel feed in the BioPower 5 CHP plant, and by using the FT-IR analyzer measurements. According to the fuel sampling, the average moisture content of the wet fuel was 54.4%. In comparison, the soft-sensor estimated that the average moisture content of the fuel was 54.6%. The average moisture content of the dry fuel was 25.9%, whereas the soft-sensor estimated that the average moisture con-

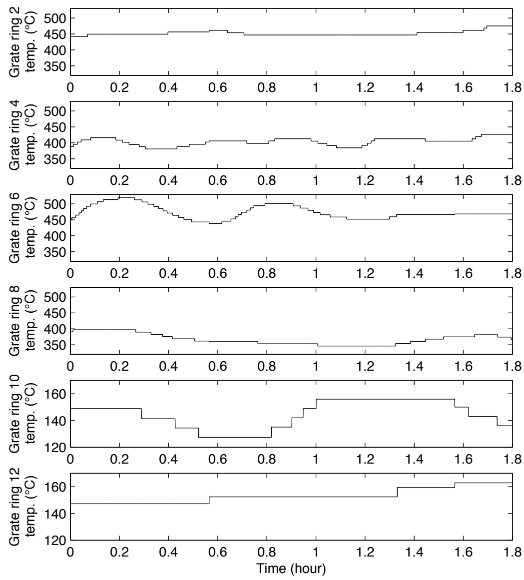

Figure 5.4. Grate temperatures during the first test. A total of six temperature measurement probes were installed radially on grate rings and these are numbered from the center (grate ring 2) to the edge of the grate (grate ring 12). (Publication II)

tent of the fuel was 27%. This shows that the estimations of the fuel moisture soft-sensor and the values of the moisture samples were very similar. The standard error of performance (SEP) of the soft-sensor is 3.6% when compared with the FT-IR that has the combined error of 3.3% (Bak and Clausen, 2002).

The dynamic behavior of the fuel moisture soft-sensor was studied in the BioPower CHP plant by producing a step function of moisture in the flue gases by feeding portions of dry biomass in between portions of wet fuel. The results, presented in Figures 5.1 to 5.4, show that the fuel moisture soft-sensor responded to the step changes within 1 minute compared with the FT-IR analyzer measurements. In addition, the fuel moisture soft-sensor showed no sign of hysteresis, responding equally to both positive and negative changes in moisture content. This verifies that this method of detecting varying moisture is accurate and responsive enough so that it can be used to control air and fuel feeds.

The greater amount of dry fuel used in the second and the third tests caused fluctuation in the process variables. However, the same accuracy and dynamic behavior were achieved in comparison with the first test as presented in Publication II.

5.2 Identification and validation of the BioGrate combustion model

The identification of the model of the water evaporation (Equation (4.22)) and the thermal decomposition of dry fuel (Equation (4.21)) was conducted using the measurements from the BioPower 5 CHP plant. The thermal decomposition model of the dry fuel was split into the identification of the two submodels: models for the current mass of the dry biomass in Equation (4.20) and thermal decomposition rate in Equation (4.21). The aim of the identification was to determine the model parameters c_{wev}, $c_{w,in}$, c_{td}, c_{ds}, $c_{ds,in}$, and c_{thd}.

The input variables, stoker speed, primary air flow, and fuel bed pressure were taken from the process data. From a total eight pressure sensors available, the measurements of the fifth sensor – from the center of the grate where the dry fuel locates – were collected and used for measuring the fuel height. The thermal decomposition of the dry fuel was calculated according to Equation (4.10) and all samples were recorded at one second intervals. The same arrangements as described in Section 5.1.1 were used to determine the fuel moisture content in the feed and in the flue gases and the composition of fuel.

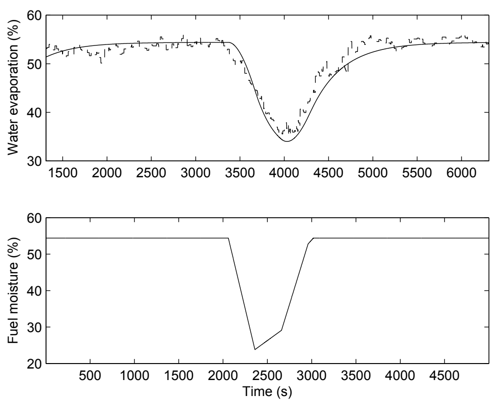

Figure 5.5. The measured (dashed line) and estimated (solid line) water evaporation, and input parameter, the moisture content of fuel feed in the identification. The delay between input and output variables is 20 minutes. (Publication III)

Fig. 5.5 shows the estimated and measured water evaporation values. The time delay t_d in Equation (4.23) between the samples taken just before the stoker screw to the point were the water starts to evaporate was

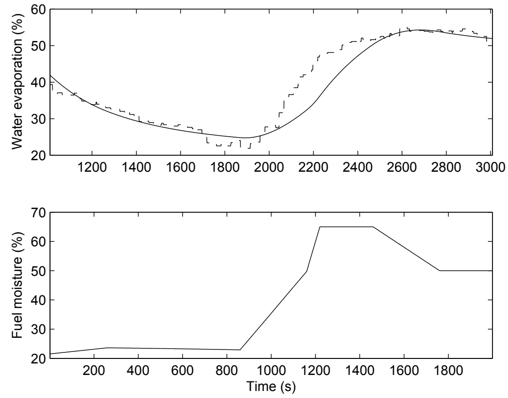

Figure 5.6. The measured (dashed line) and estimated (solid line) water evaporation, and the input parameter, the moisture content of fuel feed in the validation. The delay between input and output variables is 17 minutes. (Publication III)

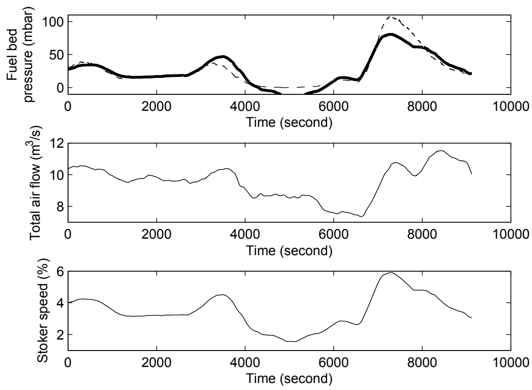

Figure 5.7. The model output variable, fuel bed pressure, and the model input variables, stoker speed and primary air in the identification. (Publication IV)

20 min. The model performance is next illustrated in Fig. 5.6. The identified model works well also on the validation data series. The time delay t_d was 17 min, due to the double amount of dry biomass fuel used in the validation tests compared with the identification. More detailed results can be found in Publication III.

Fig. 5.7 shows the estimated and measured fuel bed pressure and the inputs: total air flow, and stoker speed. The validation of the identified model was performed on another measurement series. The performance of the model for the validation data is shown in Fig. 5.8. The identified model also works well using the validation data series.

The thermal decomposition rates for different primary air flow rates and different fuel bed pressures are shown in Fig. 5.9. These results illustrate

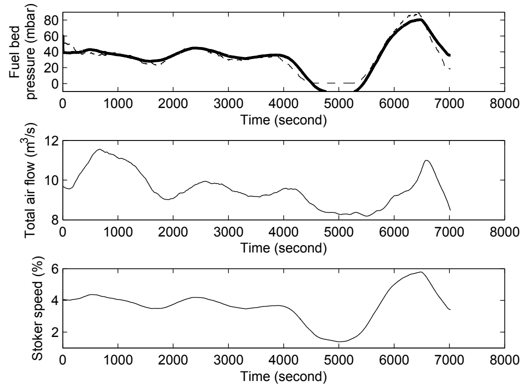

Figure 5.8. The model output variable, fuel bed pressure, and the model input variables, stoker speed and primary air in the validation. (Publication IV)

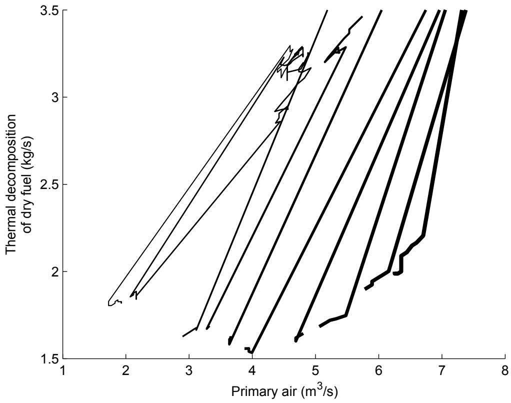

Figure 5.9. Thermal decomposition rates for different primary air values with the fuel bed pressures (from thinnest to thickest line) 10-12 mbar, 15-17 mbar, 50-52 mbar, 70-72 mbar, 80-82 mbar, 85-87 mbar, 90-92 mbar, 95-97 mbar, 98-100 mbar, and 100-102 mbar. (Publication IV)

that an increase in fuel bed pressure requires an increase in primary air flow to maintain the same thermal decomposition rate. In addition, the amount of primary air required grows almost linearly, showing the behavior as presented in Equation (4.21). More detailed results are presented in Publication IV.

5.3 Performance validation of the MPC strategy for the BioGrate boiler

5.3.1 Description of the simulated process environment

To test the MPC strategy developed in Section 4.2.5.2.2, a simulation model of the BioGrate boiler was built and the code for the MPC was developed in the MATLAB environment (Publication I). The models included the combustion model and the drum model for the BioGrate boiler, including the parameters identified in Section 5.2.

5.3.2 Test results of the MPC strategy for the BioGrate boiler

The MPC strategy was compared with the currently used control strategy in a MATLAB programming environment. The integrating disturbance states η_k were 0.047, 0.072 and 4.8975 for the model of thermal decomposition of fuel, the pressure model, and the water evaporation model, respectively. These were determined by calculating the variance of the prediction errors in the system identification and measurement disturbances v_k were approximately 1 %. The input limits were $u_{1,min} = 0$, $u_{1,max} = 5$, $\Delta u_{1,min} = -0.03$, and $\Delta u_{1,max} = 0.03$ [kg/s] for the stoker speed; $u_{2,min} = 0$, $u_{2,max} = 8$, $\Delta u_{2,min} = -0.03$, and $\Delta u_{2,max} = 0.03$ [kg/s] for the primary air. The output limits were $y_{1,min} = 0$, $y_{1,max} = 1$ [m] for the fuel bed height; and $y_{2,min} = 0$, $y_{2,max} = 55$ [bar] for the drum pressure. The MPC was tuned with:

$$Q_z = \begin{bmatrix} 0.1 & 0 \\ 0 & 0.1 \end{bmatrix} \quad \text{and} \quad Q_u = \begin{bmatrix} 0.1 & 0 \\ 0 & 0.1 \end{bmatrix}$$

In the first simulation test, the moisture content in the fuel feed was changed from 54% to 65% while the steam demand was 14 MW. The settling time of the drum pressure in the current (original) control strategy was about 2h (Fig. 5.10), whereas the change in the moisture content had no effect on the drum pressure when using the MPC strategy, as shown in Fig. 5.11. The MPC strategy employs the water evaporation model (Fig. 5.12) and gradually increases the primary air flow rate, preventing disturbances in the drum pressure.

In the second simulation test, the steam demand was changed from 12 MW to 16 MW while the moisture content in the fuel feed was kept at 57%.

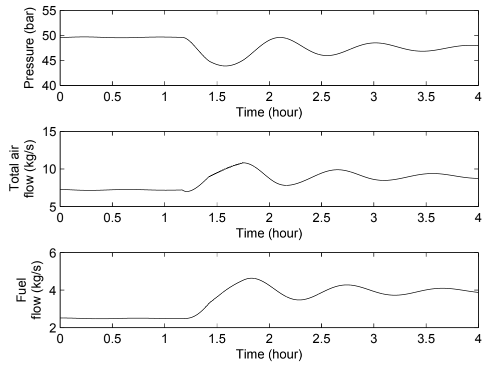

Figure 5.10. The original control strategy: Responses of the air flow, fuel flow, and pressure to a change in the moisture content of the fuel flow

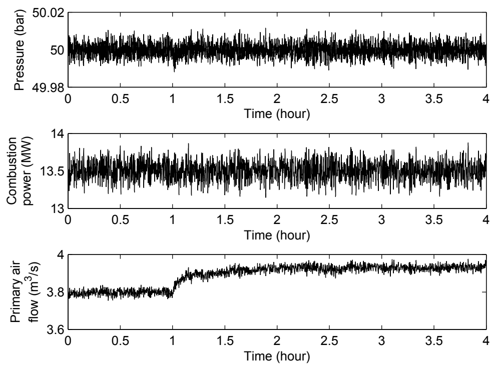

Figure 5.11. MPC strategy: Responses of the drum pressure, combustion power, and primary air flow to a change in the moisture content of the fuel flow. (Publication IV)

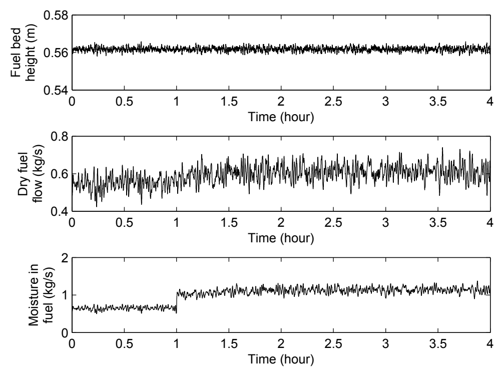

Figure 5.12. MPC strategy: Responses of the fuel bed height, dry fuel flow, and moisture in the fuel to a change in the moisture content of the fuel flow. (Publication IV)

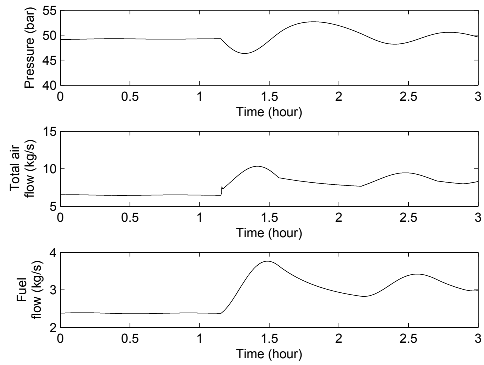

Figure 5.13. The original control strategy: Responses of the air flow, fuel flow, and pressure to a change in the steam demand

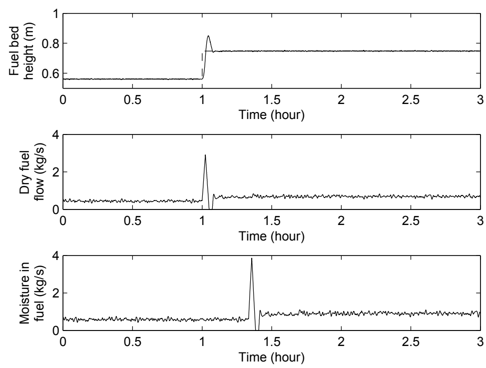

Figure 5.14. MPC strategy: Responses of fuel bed height, dry fuel flow, and moisture in the fuel to a change in the steam demand. (Publication IV)

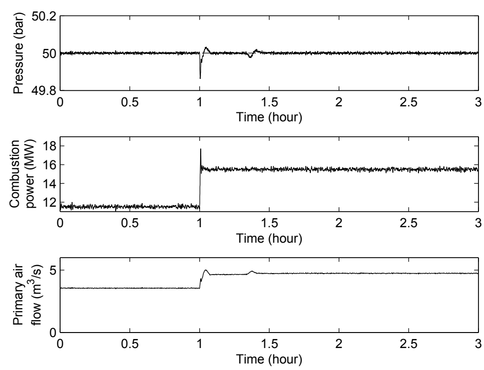

Figure 5.15. MPC strategy: Responses of the drum pressure, combustion power, and primary air flow to a change in the steam demand. (Publication IV)

With the original control strategy, the change in the steam demand again caused strong oscillations (Fig. 5.13). With the MPC strategy, the settling time of the drum pressure is only 2 minutes, as shown in Figs. 5.14-5.15. The error of the target pressure compared with the measured pressure is due to the feed-forward compensation from the steam flow in the original control strategy.

The reason for the fast settling time of 2 minutes in the response of the developed MPC strategy is that the fuel bed is controlled independently from the combustion power. This fast response is then achieved by manipulating the primary air flow rate while keeping the fuel bed height at a desired level. The combustion power was calculated by utilizing the fuel moisture soft-sensor and oxygen consumption calculations for water evaporation and thermal decomposition of dry fuel respectively. More detailed results are presented in Publication IV.

5.4 Performance validation of the FTMPC for the BioGrate boiler

5.4.1 Description of the simulated process environment

The same model presented in Section 5.3 was used to validate the FTMPC for the BioPower 5 CHP process. Additionally, the FTMPC presented in Section 4.2 was developed.

5.4.2 Test results of the FTMPC for the BioGrate boiler

To demonstrate the effectiveness of the proposed FTMPC strategy, the performance of the FTMPC was evaluated using the BioGrate boiler simulator in a MATLAB environment.

The input limits were $u_{1,min} = 0$, $u_{1,max} = 4$, $\Delta u_{1,min} = -0.03$, and $\Delta u_{1,max} = 0.03$ [kg/s] for the stoker speed; $u_{2,min} = 0$, $u_{2,max} = 4$, $\Delta u_{2,min} = -0.03$, and $\Delta u_{2,max} = 0.03$ [kg/s] for the primary air.

In the nominal case, the output limits were $y_{1,min} = 0.2$, $y_{1,max} = 1$ [m] for the fuel bed height; and $y_{2,min} = 0$, $y_{2,max} = 55$ [bar] for the drum pressure.

$$\mathbf{Q}_{z,1} = \begin{bmatrix} 0.1 & 0 \\ 0 & 0.1 \end{bmatrix} \quad \text{and} \quad \mathbf{Q}_{u,1} = \begin{bmatrix} 0.1 & 0 \\ 0 & 0.1 \end{bmatrix}$$

In the reconfiguration, the output limits were $y_{1,min} = 0.2$, $y_{1,max} = 1$ [m] for the fuel bed height; $y_{2,min} = 0$, $y_{2,max} = 30$ [MW] for the combustion power; and $y_{3,min} = 0$, $y_{3,max} = 55$ [bar] for the drum pressure.

$$\mathbf{Q}_{z,2} = \begin{bmatrix} 0.001 & 0 & 0 \\ 0 & 0.001 & 0 \\ 0 & 0 & 0.1 \end{bmatrix} \quad \text{and} \quad \mathbf{Q}_{u,2} = \begin{bmatrix} 0.1 & 0 \\ 0 & 0.1 \end{bmatrix}$$

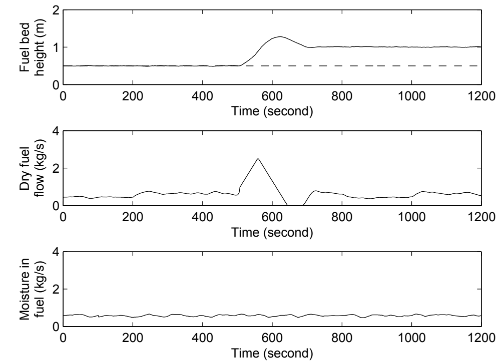

Figure 5.16. Responses of the moisture in fuel, dry fuel flow, and fuel bed height to 100% bias fault in the fuel bed height sensor without the FTMPC active. (Publication V)

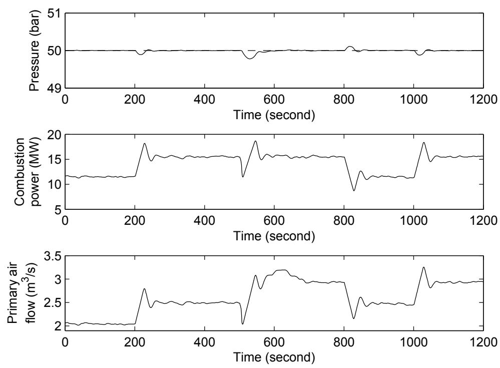

Figure 5.17. Responses of the pressure, combustion power, and primary air flow to 100% bias fault in the fuel bed height sensor without the FTMPC active. (Publication V)

The first test scenario had a downward step-shaped fault in the fuel bed height measurement of 100% of the nominal value and the power demand was changed from 12 MW to 16 MW after 200 seconds. The fault was introduced into the fuel bed height measurement after 500 seconds. Then, the power demand was changed from 16 MW to 12 MW during the time period of 800 - 1000 seconds. As it can be seen from the Figs. 5.16-5.19, the fault resulted in the high values of the primary air and the fuel bed

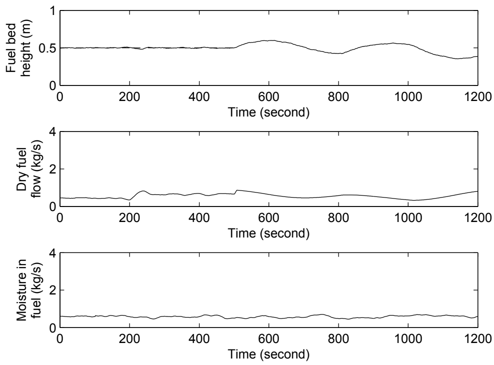

Figure 5.18. Responses of the moisture in fuel, dry fuel flow, and fuel bed height to 100% bias fault in the fuel bed height sensor with the FTMPC active. (Publication V)

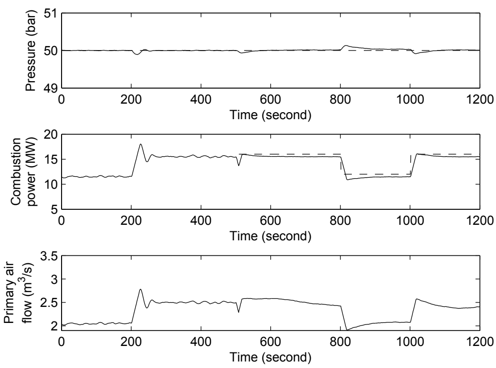

Figure 5.19. Responses of the pressure, combustion power, and primary air flow to 100% bias fault in the fuel bed height sensor with the FTMPC active. (Publication V)

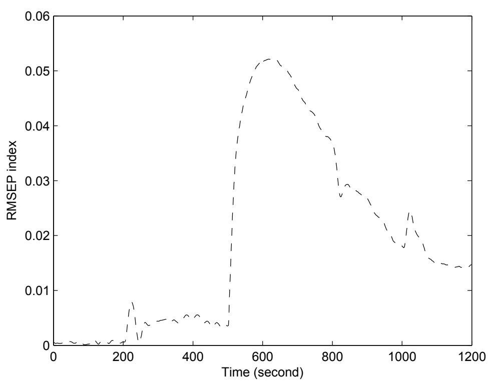

Figure 5.20. Scenario 1: RMSEP index of fuel bed height state of MPC 1 and MPC 2. (Publication V)

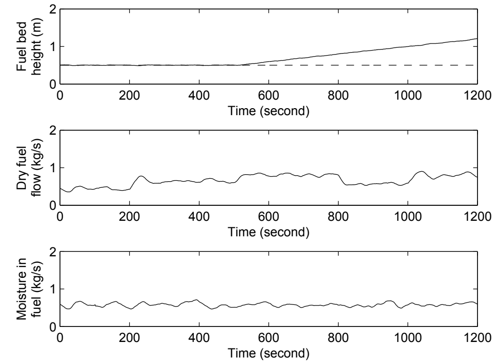

Figure 5.21. Responses of the moisture in fuel, dry fuel flow, and fuel bed height to drift fault in the fuel bed height sensor without the FTMPC active. (Publication V)

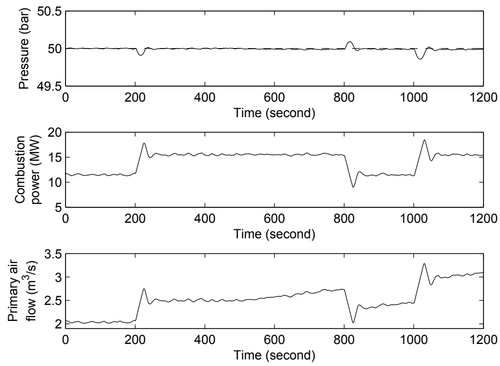

Figure 5.22. Responses of the pressure, combustion power, and primary air flow to drift fault in the fuel bed height sensor without the FTMPC active. (Publication V)

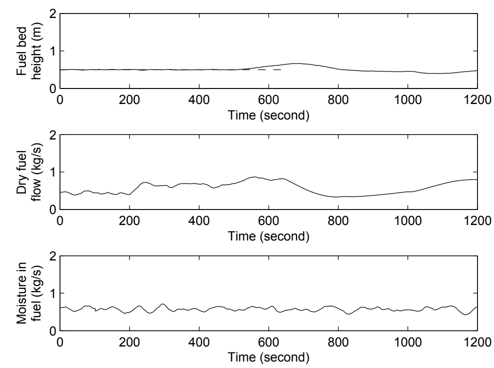

Figure 5.23. Responses of the moisture in fuel, dry fuel flow, and fuel bed height to drift fault in the fuel bed height sensor with the FTMPC active. (Publication V)

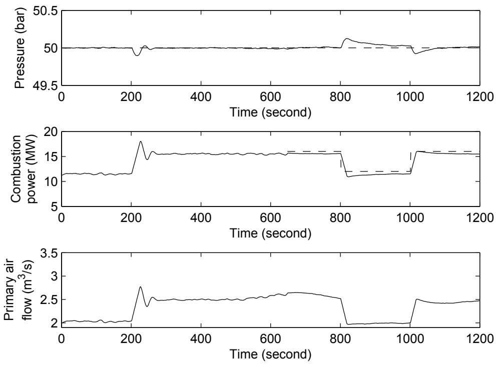

Figure 5.24. Responses of the pressure, combustion power, and primary air flow to drift fault in the fuel bed height sensor with the FTMPC active. (Publication V)

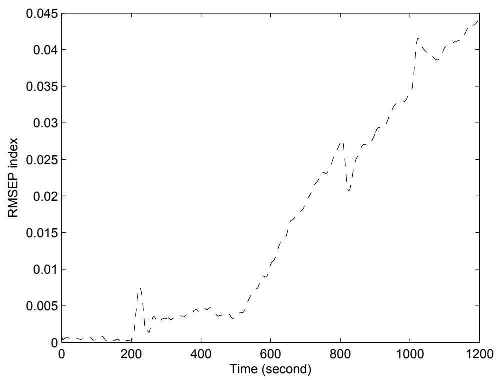

Figure 5.25. Scenario 2: RMSEP index of fuel bed height state of MPC 1 and MPC 2. (Publication V)

height. Fig. 5.20 shows the RMSEP index of the different fuel bed height state of MPC 1 and MPC 2.

In the second test scenario, the power demand was again changed from 12 MW to 16 MW after 200 seconds. The effect of a ramp-shaped fault in the fuel bed height on the closed loop performance of the system was evaluated with and without the FTMPC strategy active. A ramp-shaped fault was introduced into the fuel bed height measurement, starting from the time step 500 seconds. Then, the power demand was changed from 16 MW to 12 MW during a time period of 800 - 1000 seconds. As it can be seen from the Figs. 5.21-5.24, without the FTMPC the drift fault had the effect that both the primary air and the fuel bed height started to increase rapidly. With the FTMPC, both the primary air and the fuel bed height remained within their normal operation limits, thus improving the reliability of the control system. Compared with the first test scenario, the detection of the ramp-shaped fault was delayed as shown in Fig. 5.25.

5.5 Economic evaluation of the FTMPC for the BioGrate boiler

This section discusses the economic benefits of the enhanced control strategy addressing the problem of variations in fuel quality, described in Section 1.1. Several cases are reported in Section 5.3.2, which are used to evaluate the economic benefits of the enhanced control strategy over the current strategy. In the first case, the fuel moisture content was changed by 11 %, which caused a deviation of 5 bars in the drum pressure and a power loss of 3 MWh while using the current strategy. Note that the deviations in the steam drum pressure exceeding 6 bars leads to turbine shutdowns that in general causes almost 50% of the total energy production losses. With the enhanced control strategy, no effects on the power generation and the drum pressure were observed in simulations under the same scenario. In addition, with the enhanced strategy, the deviations in the drum pressure are kept below the safety limits, and therefore, the turbine shutdowns are completely avoided.

The developed FTMPC incorporates the fuel bed height sensor into the control strategy that allows to maintain the optimal ratio of the primary and secondary air flow rates. Gölles et al. (2014) showed that keeping this optimal ratio leads to the reduction of harmful particulate matter emission by 20% and CO emissions by 3 times compared with the conventional control strategy.

6. Conclusions

In this thesis, the FTMPC strategy considering fuel quality and fuel moisture content has been developed for the BioPower 5 CHP process. First, the BioGrate process and its control strategy were presented. Then, a literature review in state-of-the-art control of grate boilers was presented. Second, the FTMPC for the BioGrate boiler and its modules were developed: The developed MPC utilizes combustion power and moisture soft-sensors and models of the water evaporation and thermal decomposition of dry fuel. Furthermore, the developed FTMPC accommodates the fault in a fuel bed height sensor by active controller reconfiguration. The fuel moisture soft-sensor was tested at the BioPower 5 CHP plant. Validation of models of the water evaporation and thermal decomposition of dry fuel was conducted using the measurements of the BioPower 5 CHP plant. Then the MPC strategy was compared with the currently used control strategy. Finally, the performance of the FTMPC was evaluated with the simulated BioGrate boiler.

The hypothesis presented in Chapter 1 is: The availability and profitability of the BioPower 5 CHP process are improved by integration of fuel moisture content and combustion power estimations into a fault-tolerant model predictive control (FTMPC) scheme. This hypothesis has been verified by the results acquired in testing the fuel moisture soft-sensor by the industrial tests in the BioPower 5 CHP plant in Section 5.1, testing the proposed MPC with the simulated BioGrate boiler in Section 5.3, and testing the proposed FTMPC with the simulated BioGrate boiler in Section 5.4.

First, the results showed that developed fuel moisture soft-sensor predicts the moisture content in the furnace with a good precision, and that the method was able to detect variations in the moisture content of the furnace within seconds. The standard error of performance (SEP) of the soft-sensor is 3.6%. Second, it was shown that water evaporation and thermal decomposition of dry fuel can be estimated by utilizing fuel moisture soft-sensor and oxygen consumption calculations respectively. The fast settling time of 2 minutes in the response of the developed MPC strategy was achieved by regulating the primary air while keeping the fuel bed height at a desired level. In comparison, the settling time in the response of the currently used control strategy was 2 h. On the basis of the simulation results, the proposed FTMPC was able to counter the most typical fault in the BioPower 5 CHP plant that is caused by the unknown fuel quality and the status of the furnace (amount of fuel in the furnace). Therefore, the performance and the profitability of the BioPower 5 CHP plant would be significantly enhanced if such an FTMPC strategy is implemented.

The FTMPC outlined in this thesis has been developed for the BioGrate process. Nevertheless, due to its general applicability it could be used for other similar processes and thus the same advantages could be achieved in other plants regardless of the fuels and burning methods used. The greatest benefits can, however, be attained in plants fuelled with inhomogenous fuels, such as peat, coal, bark and waste. In the future, the FTMPC can also play a major role in controlling, for example, the next generation of small-scale biomass boilers.

In this thesis, a model predictive fault tolerant scheme for the BioGrate boiler was reported, where the model was identified using the industrial test results. The next step in this direction is to experimentally validate the effectiveness of the developed FTMPC scheme by integrating it in the industrial automation system. In addition, the applicability of the developed FTMPC scheme is worth investigating for faults occurring in a wider class of boilers.

Bibliography

Anon (2014). *BioGrate Technology*. Available from: http://www.valmet.com [Accessed 1 June 2014].

Axrup, L., Markides, K., and Nilsson, T. (2000). Using miniature diode array NIR spectrometers for analysing wood chips and bark samples in motion. *Journal of Chemometrics*, 14(5-6):561–572.

Bak, J. and Clausen, S. (2002). FTIR emission spectroscopy methods and procedures for real time quantitative gas analysis in industrial environments. *Measurement Science and Technology*, 13(2):150–156.

Bauer, R., Gölles, M., Brunner, T., Dourdoumas, N., and Obernberger, I. (2010). Modelling of grate combustion in a medium scale biomass furnace for control purposes. *Biomass and Bioenergy*, 34(4):417–427.

Blasi, C. D. (2000). Dynamic behaviour of stratified downdraft gasifiers. *Chemical Engineering Science*, 55(15):2931–2944.

Boriouchkine, A., Sharifi, V., Swithenbank, J., and Jämsä-Jounela, S.-L. (2014). A study on the dynamic combustion behavior of a biomass fuel bed. *Fuel*, 135:468–481.

Edlund, K., Bendtsen, J. D., and Jørgensen, J. B. (2011). Hierarchical model-based predictive control of a power plant portfolio. *Control Engineering Practice*, 19(10):1126–1136.

Effenberger, H. (2000). *Dampferzeuger*. Springer-Verlag Berlin Heidelberg New York, pp 20-69.

Frank, P. M., Ding, S. X., and Marcu, T. (2000). Model-based fault diagnosis in technical processes. *Transactions of the institute of measurement and control*, 22(1):57–101.

Gölles, M., Bauer, R., Brunner, T., Dourdoumas, N., and Obernberger, I. (2011). Model based control of a biomass grate furnace. In *Proceedings of the 9th European conference on industrial furnaces and boilers*, pages 1–10, Estoril.

Gölles, M., Reiter, S., Brunner, T., Dourdoumas, N., and Obernberger, I. (2014). Model based control of a small-scale biomass boiler. *Control Engineering Practice*, 22:94–102.

Gómez, M. A., Porteiro, J., Patiño, D., and Míguez, J. L. (2014). CFD modelling of thermal conversion and packed bed compaction in biomass combustion. *Fuel*, 117(Part A):716–732.

Haghani, A., Jeinsch, T., and Ding, S. X. (2014). Quality-Related Fault Detection in Industrial Multimode Dynamic Processes. *IEEE Transactions on Industrial Electronics*, 61(11):6446–6453.

Hermansson, S., Lind, F., and Thunman, H. (2011). On-line monitoring of fuel moisture-content in biomass-fired furnaces by measuring relative humidity of the flue gases. *Chemical Engineering Research and Design*, 89(11):2470–2476.

Incropera, F. P., DeWitt, D. P., Bergman, T. L., and Lavine, A. S. (2007). *Fundamentals of Heat and Mass Transfer*. John Wiley & Sons, pp 501-530.

Jaakkola, P. T., Vahlman, T. A., Roos, A. A., Saarinen, P. E., and Kauppinen, J. K. (1998). On-line Analysis of Stack Gas Composition by a Low Resolution FT-IR Gas Analyzer. *Water, Air, and Soil Pollution*, 101(1-4):79–92.

Jegoroff, M., Leino, T., and Heiskanen, V.-P. (2013). New method for controlling combustion in a grate boiler. In Kovács, J. and Hultgren, M., editors, *The proceedings of the 18th Nordic Process Control Workshop*, Oulu, Available from: http://www.nt.ntnu.no/users/skoge/prost/proceedings/npcw2013/18th_NPCW_proceedings.pdf.

Johansson, R., Thunman, H., and Leckner, B. (2007). Influence of intraparticle gradients in modeling of fixed bed combustion. *Combustion and Flame*, 149(1-2):49–62.

Kallioniemi, J. (2008). *Utilising process monitoring methods in BioPower plant process*. Master's thesis, Helsinki University of Technology, Espoo, pp 21-40.

Kettunen, M. and Jämsä-Jounela, S.-L. (2011). Data-Based, Fault-Tolerant Model Predictive Control of a Complex Industrial Dearomatization Process. *Industrial & Engineering Chemistry Research*, 50(11):6755–6768.

Kohonen, T. (1990). The self-organizing map. *Proceedings of the IEEE*, 78:1464–1480.

Kortela, J. and Jämsä-Jounela, S.-L. (2010). Fuel quality soft-sensor for control strategy improvement of the Biopower 5 CHP plant. In *Proceedings of the Conference on Control and Fault-Tolerant Systems (SysTol'10)*, pages 221–226, Nice.

Kortela, U. and Lautala, P. (1982). A new control concept for a coal power plant. *Control Science and Technology for the Progress of Society*, 6:3017–3023.

Kortela, U. and Marttinen, A. (1985). Modelling, Identification and Control of a Grate Boiler. In *Proceedings of the 1985 American Control Conference*, pages 544–549, Boston.

Lehtomäki, K., Kortela, U., and Luukkainen, J. (1982). New estimation and control methods for fuel power in peat power plants. *Control Science and Technology for the Progress of Society*, 6:3039–3044.

Leão, R. P. S., Barroso, G. C., Sampaio, R. F., Almada, J. B., Lima, C. F. P., Rego, M. C. O., and Antunes, F. L. M. (2011). The future of low voltage networks: Moving from passive to active. *International Journal of Electrical Power & Energy Systems*, 33(8):1506–1512.

Leskens, M., van Kessel, L. B. M., and Bosgra, O. H. (2005). Model predictive control as a tool for improving the process operation of MSW combustion plants. *Waste Management*, 25(8):788–798.

Li, W., Yue, H. H., Valle-Cervantes, S., and Qin, S. J. (2000). Recursive pca for adaptive process monitoring. *Journal of Process Control*, 10:471–486.

Lu, S. (1999). Dynamic modelling and simulation of power plant systems. *Proceedings of the Institution of Mechanical Engineers, Part A: Journal of Power and Energy*, 213(1):7–22.

Lu, S. and Hogg, B. W. (2000). Dynamic nonlinear modelling of power plant by physical principles and neural networks. *International Journal of Electrical Power & Energy Systems*, 22(1):67–78.

Maciejowski, J. M. (2002). *Predictive Control with Constraints*. Prentice Hall, Harlow, pp 36-150.

Nordell, A. and Vikterlöf, K. J. (2000). *Measurements of moisture content in wood fuels with dual energy X-ray*. Värmeforsk, Stockholm, Available from: http://www.varmeforsk.se [Accessed 1 June 2014].

Nyström, J. and Dahlquist, E. (2004). Methods for determination of moisture content in woodchips for power plants—a review. *Fuel*, 83(7-8):773–779.

Okamura, S. and Zhang, Y. (2000). New method for moisture content measurement using phase shifts at two microwave frequencies. *Journal of Microwave Power and Electromagnetic Energy*, 35(3):175–178.

Paces, N., Voigt, A., Jakubek, S., Schirrer, A., and Kozek, M. (2011). Combined Control of Combustion Load and Combustion Position in a Moving Grate Biomass Furnace. In *Proceedings of the 19th European Conference on Control & Automation (MED)*, pages 1447–1452, Corfu.

Pannocchia, G. and Rawlings, J. B. (2003). Disturbance Models for Offset-Free Model-Predictive Control. *AIChE Journal*, 49(2):426–437.

Patwardhan, S. C., Manuja, S., Narasimhan, S., and Shah, S. L. (2006). From data to diagnosis and control using generalized orthonormal basis filters. Part II: Model predictive and fault tolerant control. *Journal of Process Control*, 16(2):157–175.

Prakash, J., Patwardhan, S. C., and Narasimhan, S. (2002). A Supervisory Approach to Fault-Tolerant Control of Linear Multivariable Systems. *Industrial & Engineering Chemistry Research*, 41(9):2270–2281.

Qin, S. J. (1998). Recursive pls algorithms for adaptive data modeling. *Computers and Chemical Engineering*, 22(4):503–514.

Rosenberg, E., Schatvet, J., and Høydal, K. (2001). In-kiln measurements of moisture content in timber at moelven våler as. In *Proceedings of the 3rd European Cost E15 Workshop on Wood Drying : With the Theme Softwood Drying to Meets Needs of Further Processing and Specific End-uses*, pages 1–9, Helsinki.

Saastamoinen, J. J., Taipale, R., Horttanainen, M., and Sarkomaa, P. (2000). Propagation of the ignition front in beds of wood particles. *Combustion and Flame*, 123(1-2):214–226.

Sourander, M., Vermasvuori, M., Sauter, D., Liikala, T., and Jämsä-Jounela, S.-L. (2009). Fault tolerant control for a dearomatisation process. *Journal of Process Control*, 19(7):1091–1102.

Ström, H. and Thunman, H. (2013). A computationally efficient particle submodel for CFD-simulations of fixed-bed conversion. *Applied Energy*, 112:808–817.

Åström, K. J. and Bell, R. D. (2000). Drum-boiler dynamics. *Automatica*, 36(3):363–378.

Thunman, H. and Leckner, B. (2001). Ignition and propagation of a reaction front in cross-current bed combustion of wet biofuels. *Fuel*, 80(4):473–481.

Thunman, H. and Leckner, B. (2003). Co-current and counter-current fixed bed combustion of biofuel—a comparison. *Fuel*, 82(3):275–283.

van der Lans, R. P., Pedersen, L. T., Jensen, A., Glarborg, P., and Dam-Johansen, K. (2000). Modelling and experiments of straw combustion in a grate furnace. *Biomass and Bioenergy*, 19(3):199–208.

Venkatasubramanian, V., Rengaswamy, R., Yin, K., and Kavuri, S. N. (2003). A review of process fault detection and diagnosis: Part I: Quantitative model-based methods. *Computers & Chemical Engineering*, 27(3):293–311.

Winterton, R. H. S. (1998). Where did the dittus and boelter equation come from? *International Journal of Heat and Mass Transfer*, 41(4-5):809–810.

Yang, Y. B., Ryu, C., Khor, A., Yates, N. E., Sharifi, V. N., and Swithenbank, J. (2005a). Effect of fuel properties on biomass combustion. Part II. Modelling approach—identification of the controlling factors. *Fuel*, 84(16):2116–2130.

Yang, Y. B., Ryu, C., Khor, A., Yates, N. E., Sharifi, V. N., and Swithenbank, J. (2005b). Fuel size effect on pinewood combustion in a packed bed. *Fuel*, 84(16):2026–2038.

Yang, Y. B., Yamauchi, H., Nasserzadeh, V., and Swithenbank, J. (2003). Effects of fuel devolatilisation on the combustion of wood chips and incineration of simulated municipal solid wastes in a packed bed. *Fuel*, 82(18):2205–2221.

Yin, C., Rosendahl, L. A., and Kær, S. K. (2008). Grate-firing of biomass for heat and power production. *Progress in Energy and Combustion Science*, 34(6):725–754.

Zhang, Y. and Jiang, J. (2008). Bibliographical review on reconfigurable fault-tolerant control systems. *Annual Reviews in Control*, 32(2):229–252.

Zheng, C., Patton, R. J., and Chen, J. (1997). Robust fault-tolerant systems synthesis via LMI. In *IFAC Safeprocess'97*, pages 347–352.

Aalto-DD 20/2015

ISBN 978-952-60-6079-8 (printed)
ISBN 978-952-60-6080-4 (pdf)
ISSN-L 1799-4934
ISSN 1799-4934 (printed)
ISSN 1799-4942 (pdf)

Aalto University
School of Chemical Technology
Department of Biotechnology and Chemical Technology
www.aalto.fi

BUSINESS +
ECONOMY

ART +
DESIGN +
ARCHITECTURE

SCIENCE +
TECHNOLOGY

CROSSOVER

DOCTORAL
DISSERTATIONS